Theoretical aspects: Isospin Effects and EOS in Nuclear Reactions

Bao-An Li

Physics & Astronomy
Texas A&M University-Commerce

Collaborators: Bao-Jun Cai, Lie-Wen Chen, Wen-Jie Xie, Jun Xu, Naibo Zhang

NSF

Office of Science
U.S. DEPARTMENT OF ENERGY

Empirical parabolic law of the EOS of cold, neutron-rich nucleonic matter

symmetry energy

Isospin asymmetry

$$E(\rho_n,\rho_p) = E_0(\rho_n=\rho_p) + E_{sym}(\rho)\left(\frac{\rho_n-\rho_p}{\rho}\right)^2 + o(\delta^4)$$

Energy per nucleon in symmetric matter

Energy in asymmetric nucleonic matter

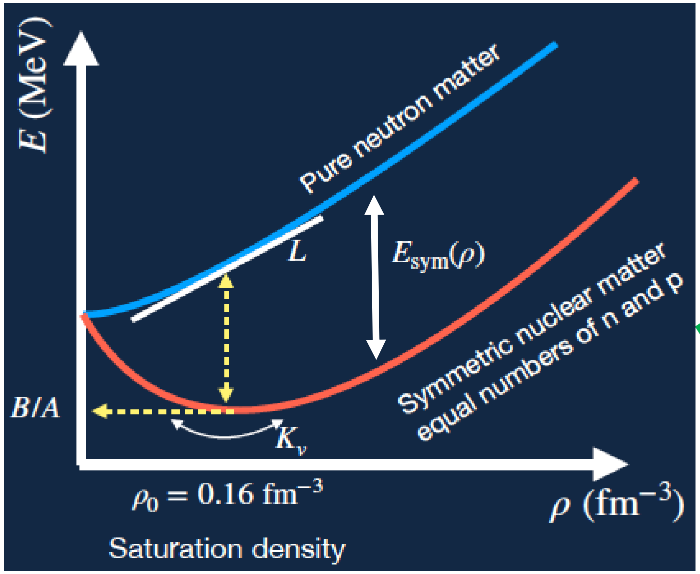

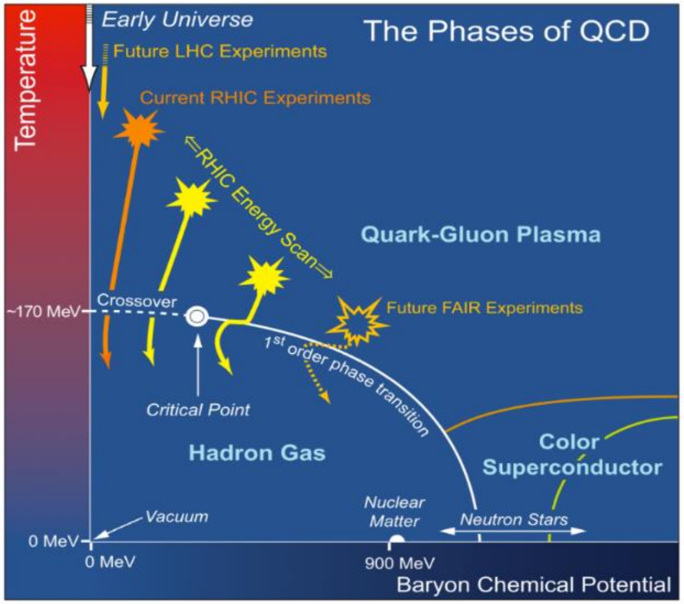

density

New opportunities

Isospin asymmetry

$\delta = (\rho_n - \rho_p)/\rho$

Isospin effects in observables of structures & collisions of neutron stars & heavy nuclei

$$E_{\mathrm{sym}}(\rho) = E_{\mathrm{sym}}(\rho_i) + \int_{\rho_i}^{\rho} \frac{P_{\mathrm{PNM}}(\rho_v) - P_{\mathrm{SNM}}(\rho_v)}{\rho_v^2} d\rho_v$$

Making a few steps in a random walk through some progresses and issues regarding

(1) The incompressibility, skewness and kurtosis of symmetric matter

(2) Nucleon effective masses in neutron-rich matter and their effects on isospin transport in nuclear reactions

(3) The curvature parameter K_{sym} and high-density nuclear symmetry energy from observables of nuclear reactions and neutron stars

Fundamental Microphysics Theories underlying each term in the EOS , what …, why …., where …how

Experimental and Observational Macrophysics underlying each observable and phenomenon, what …, why …., where …how

Empirical parameterizations

Transport model simulations of heavy-ion collisions, energy density functionals for nuclear structures, Bayesian inferences of EOS, properties of neutron stars, waveforms of gravitational waves, ….

$$E(\rho,\delta)=E_0(\rho)+E_{\rm sym}(\rho)\cdot\delta^2$$

Assuming no hadron-quark phase transition

$$E_0(\rho)=E_0(\rho_0)+\frac{K_0}{2}\left(\frac{\rho-\rho_0}{3\rho_0}\right)^2+\frac{J_0}{6}\left(\frac{\rho-\rho_0}{3\rho_0}\right)^3+\frac{Z_0}{24}\left(\frac{\rho-\rho_0}{3\rho_0}\right)^4,$$

$$E_{\rm sym}(\rho)=E_{\rm sym}(\rho_0)+\frac{L}{3}\left(\frac{\rho}{\rho_0}-1\right)+\frac{K_{\rm sym}}{18}\left(\frac{\rho}{\rho_0}-1\right)^2+\frac{J_{\rm sym}}{162}\left(\frac{\rho}{\rho_0}-1\right)^3+\mathcal{O}\left[\left(\frac{\rho}{\rho_0}-1\right)^4\right]$$

Near the saturation density $\boldsymbol{\rho}_{0,}$ they are Taylor expansions, appropriate for structure studies. Just parameterizations when applied to heavy-ion collisions and the core of neutron stars

"Current" status of the restricted EOS parameter space:

Low density: $K_0=240\pm20$, $E_{\rm sym}(\rho_0)=31.7\pm3.2$ and $L=58.7\pm28.1$ MeV

High density: $-400\le K_{\rm sym}\le100$, $-200\le J_{\rm sym}\le800$, and $-800\le J_0\le400$ MeV

Bayesian inference of high-density SNM EOS parameters from heavy-ion reaction data

	K_0	J_0	Z_0
Av	235	−200	−146
σ	30	200	1728
Min	145	−800	−5330
Max (3σ)	325	400	5038

Prior ranges of SNM EOS parameters based on theories and data available

Margueron J, Hoffmann C R and Gulminelli F 2018 PRC97, 025805 and 025806

Antic S, Chatterjee D, Carreau T and Gulminelli F 2019 J. Phys. G: Nucl. Part Phys. 46 065109

The pressure in symmetric nuclear matter

$$P(\rho) = \rho^2 \frac{\mathrm{d}E_0(\rho)}{\mathrm{d}\rho} = \frac{\rho^2}{\rho - \rho_0}\left[K_0\left(\frac{\rho-\rho_0}{3\rho_0}\right)^2 + \frac{J_0}{2}\left(\frac{\rho-\rho_0}{3\rho_0}\right)^3 + \frac{Z_0}{6}\left(\frac{\rho-\rho_0}{3\rho_0}\right)^4\right].$$

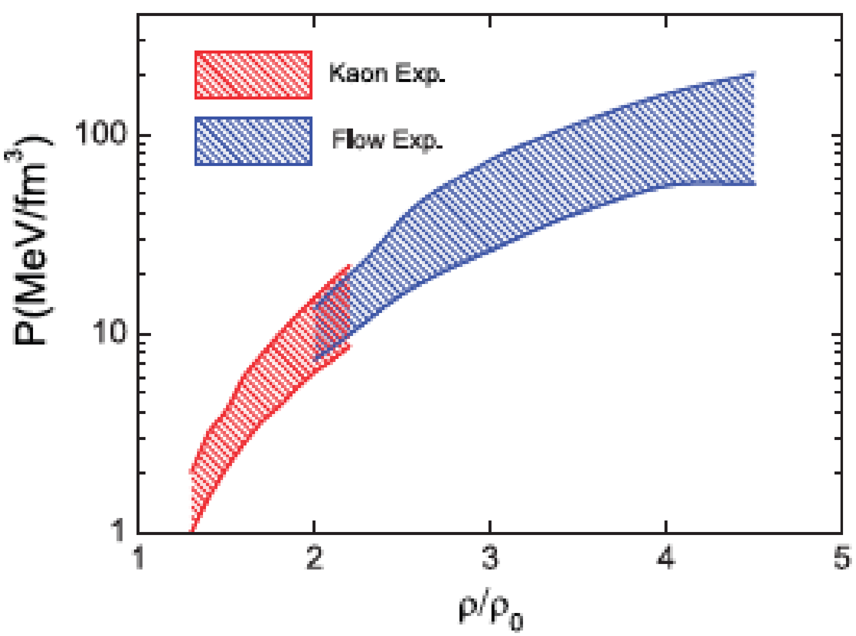

Constraints on the EOS of symmetric nuclear matter from heavy-ion collisions

Danielewicz P. I., Lacey R and Lynch W G 2002 *Science* 298 1592

Fuchs C 2006 *Prog. Part. Nucl. Phys.* 56 1

Lynch W G *et al* 2009 *Prog. Part. Nucl. Phys.* 62 427

Bayesian inference of the EOS parameters from the empirical pressure as a function of density “data”

Wen-Jie Xie and Bao-An Li
JPG 48, 025110 (2021)

Posterior PDF: $P(\mathcal{M}(K_0,J_0,Z_0)|D) = CP(D|\mathcal{M}(K_0,J_0,Z_0))P(\mathcal{M}(K_0,J_0,Z_0)),$

Prior PDF

$$P[D|\mathcal{M}(K_0,J_0,Z_0)] = \prod_{j=1}^{N} \frac{1}{\sqrt{2\pi}\sigma_{D,j}} \exp\left[-\frac{(P_{\mathrm{th},j}-P_{D,j})^2}{2\sigma_{D,j}^2}\right]$$

Likelihod function

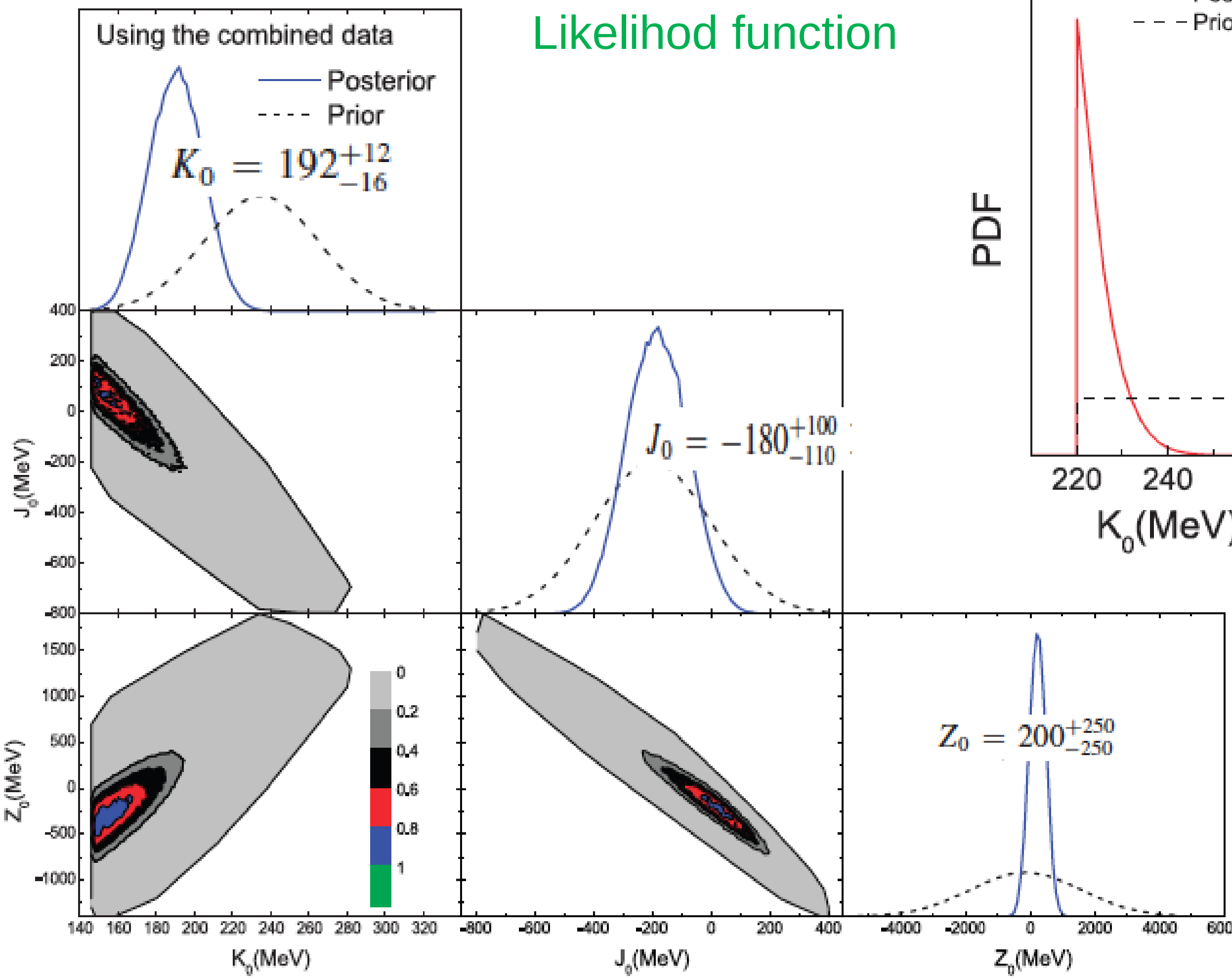

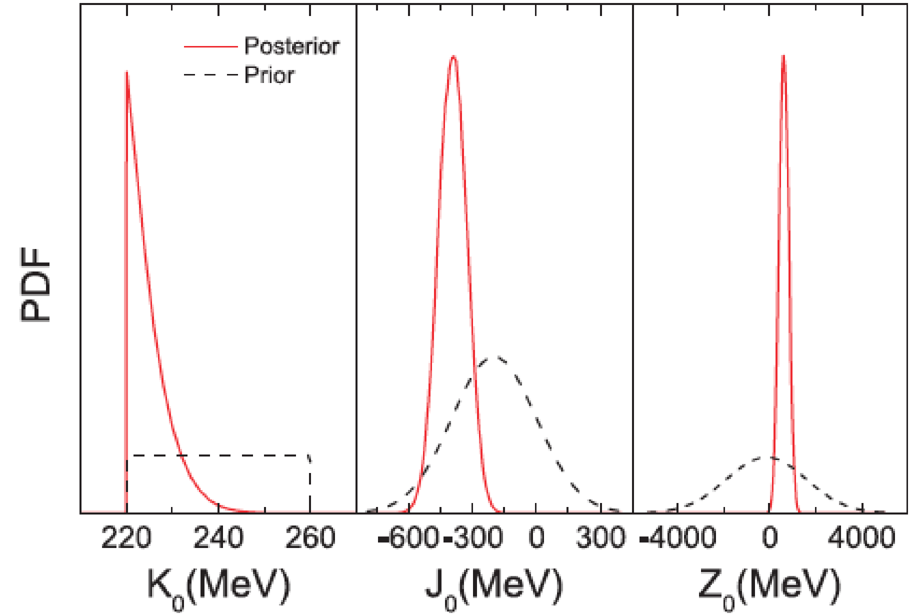

Kaon production and elliptical flow data from GSI favors a K_0 smaller than the fiducial value from ISGMR data: 240±20 MeV

A. Le Fe`vre et al., NPA945, 112 (2016).

Y.J. Wang et al., PLB778, 207 (2018)

Bayesian inference of K_0 from combined data of centroid energy and electrical Polarizability of IVGDR, n-skin, and centroid energy of ISGMR using SHF+RPA

	E_{-1} (MeV)	α_D (fm^3)	Δr_{np} (fm)	E_{ISGMR} (MeV)	E_b (MeV)	R_c (fm)
^{208}Pb-TAMU	13.46 ± 0.10	19.6 ± 0.6	0.170 ± 0.023	14.17 ± 0.28	$-7.867452 \pm 3\%$	$5.5010 \pm 3\%$
^{208}Pb-RCNP	13.46 ± 0.10	19.6 ± 0.6	0.170 ± 0.023	13.9 ± 0.1	$-7.867452 \pm 3\%$	$5.5010 \pm 3\%$
^{208}Pb-RCNP-PREXII	13.46 ± 0.10	19.6 ± 0.6	0.283 ± 0.071	13.9 ± 0.1	$-7.867452 \pm 3\%$	$5.5010 \pm 3\%$
^{120}Sn	15.38 ± 0.10	8.59 ± 0.37	0.150 ± 0.017	15.7 ± 0.1	$-8.504548 \pm 3\%$	$4.6543 \pm 3\%$

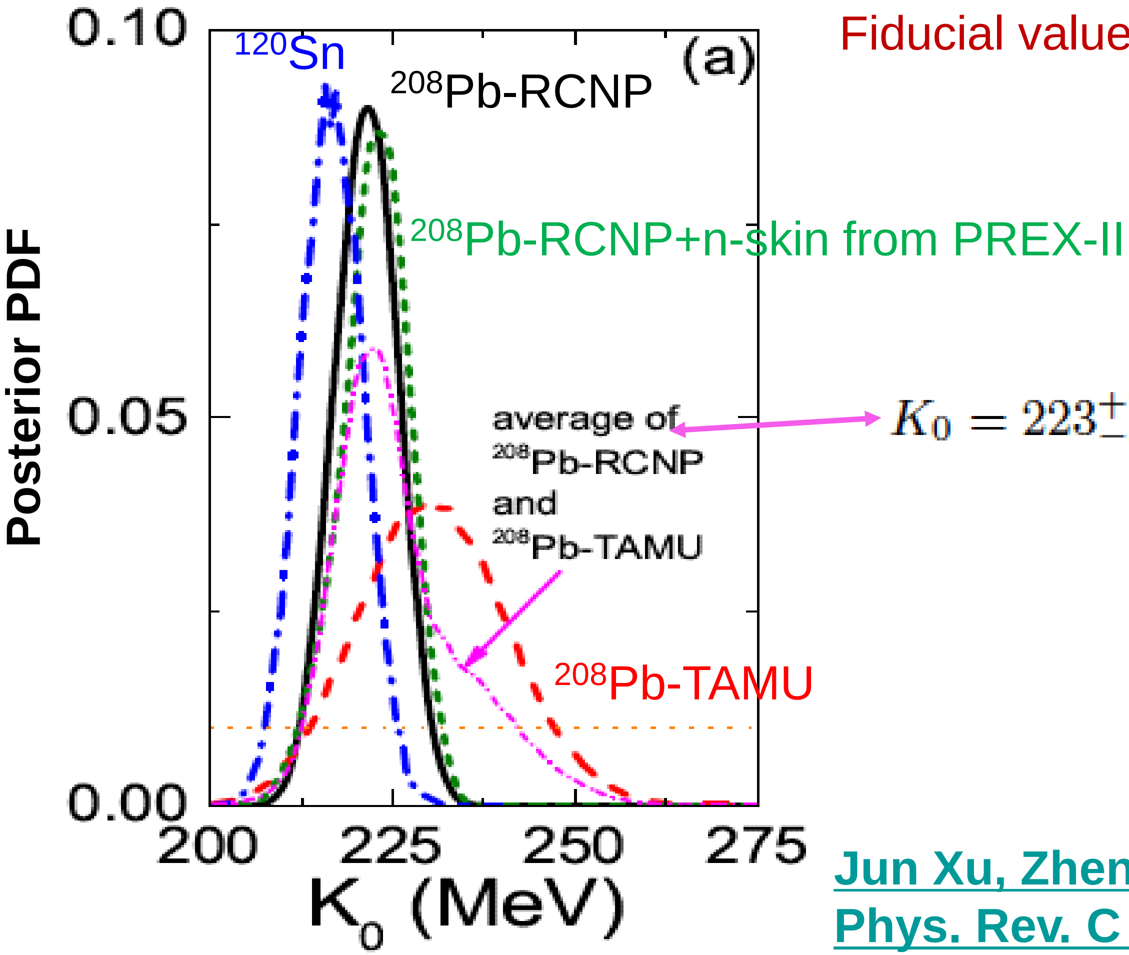

Fiducial value of K_0 since 1980: 220-260 MeV

$$K_0 = 223^{+7}_{-8} \text{ MeV at 68\% confidence level}$$

Jun Xu, Zheng Zhang and Bao-An Li, Phys. Rev. C (2021) in press, arXiv:2107.10962

The soft-tin ``puzzle”: both relativistic and non-relativistic models that well describe the ISGMR of ^{208}Pb can NOT reproduce the data of Sn isotopes

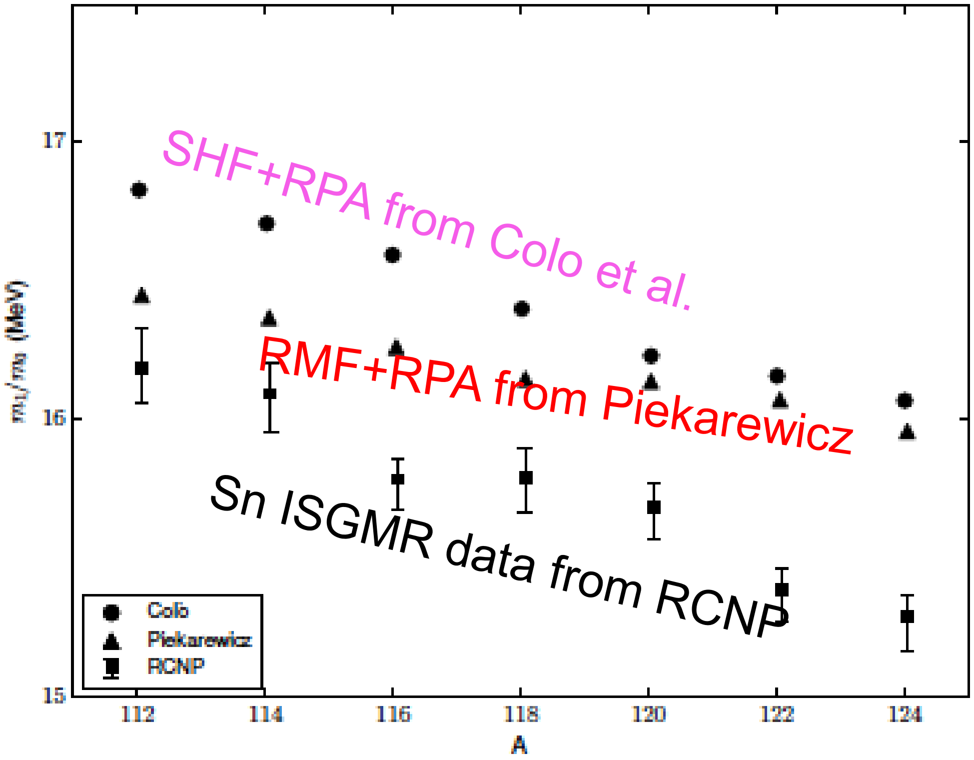

U. Garg and G. Colo, PPNP 101, 55 (2018)

The main source of the remaining uncertainty of K_0 is due to its correlation with the poorly known isospin dependence of K_A, i.e., the K_τ term

J. Colo, N. Van Giai, J. Meyer, K. Bennaceur, and P. Bonche, PRC 70, 024307 (2004).

$$E_{-1} = \sqrt{\frac{m_1}{m_{-1}}}.$$

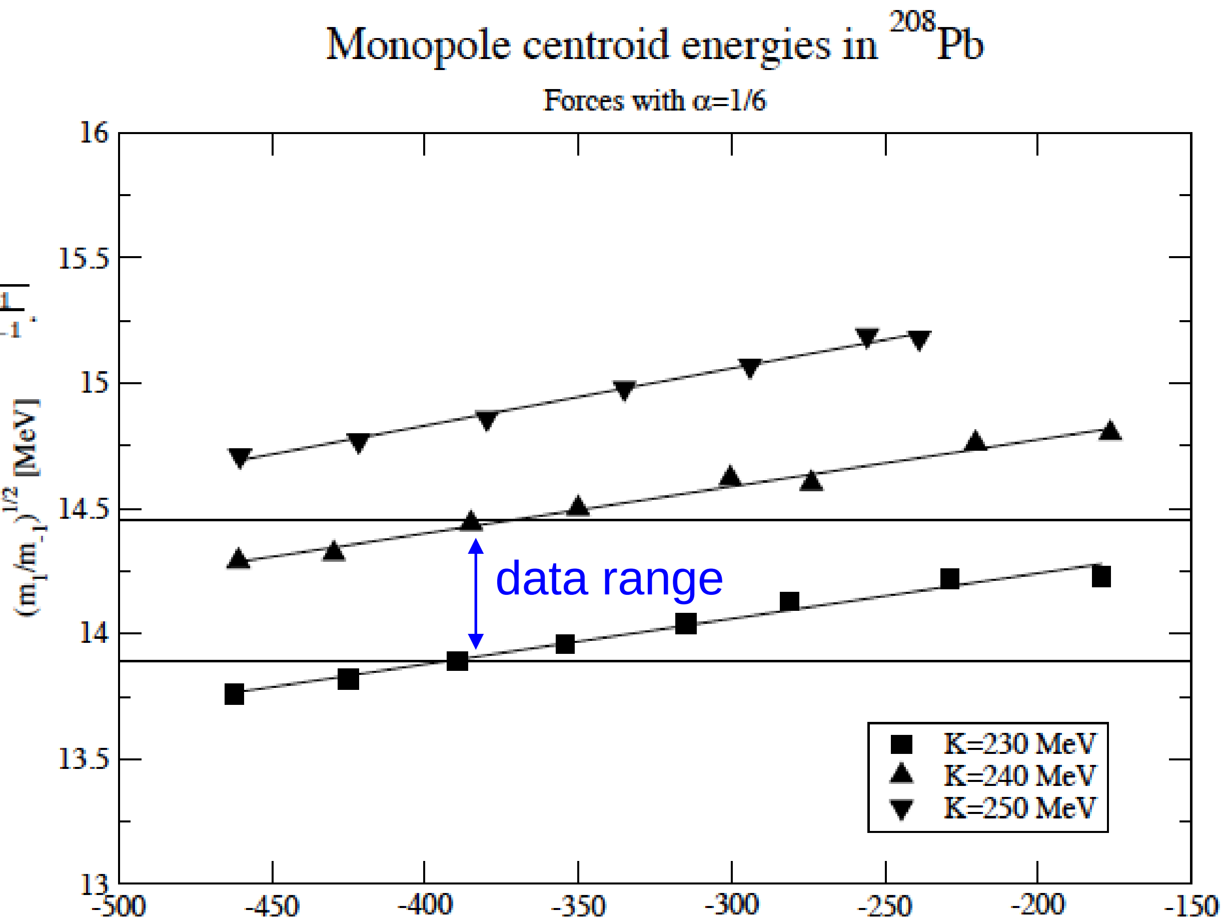

the K_τ term

Differential analysis of incompressibility in neutron-rich nuclei

Bao-An Li and Wen-Jie Xie, Phys. Rev. C 104, 034610 (2021)

$$K_A \approx K_\infty(1 + cA^{-1/3}) + K_\tau \delta^2 + K_{\rm Cou} Z^2 A^{-4/3}$$

J. P. Blaizot, Phys. Rep. 64, 171 (1980).

$$K_\tau = \left[\frac{K_{A_1}}{S_1} - \frac{K_{A_2}}{S_2} - K_{\rm Cou}\left(\frac{Z_1^2 A_1^{-4/3}}{S_1} - \frac{Z_2^2 A_2^{-4/3}}{S_2}\right)\right] \Big/ \left(\frac{\delta_1^2}{S_1} - \frac{\delta_2^2}{S_2}\right),$$

$$K_\infty = \left[\frac{K_{A_1}}{\delta_1^2} - \frac{K_{A_2}}{\delta_2^2} - K_{\rm Cou}\left(\frac{Z_1^2 A_1^{-4/3}}{\delta_1^2} - \frac{Z_2^2 A_2^{-4/3}}{\delta_2^2}\right)\right] \Big/ \left(\frac{S_1}{\delta_1^2} - \frac{S_2}{\delta_2^2}\right)$$

$$K_{\rm A} = \left(\frac{E_{\rm ISGMR}}{\hbar c}\right)^2 Mc^2 < r^2 >$$

U. Garg and G. Colo, PPNP 101, 55 (2018)

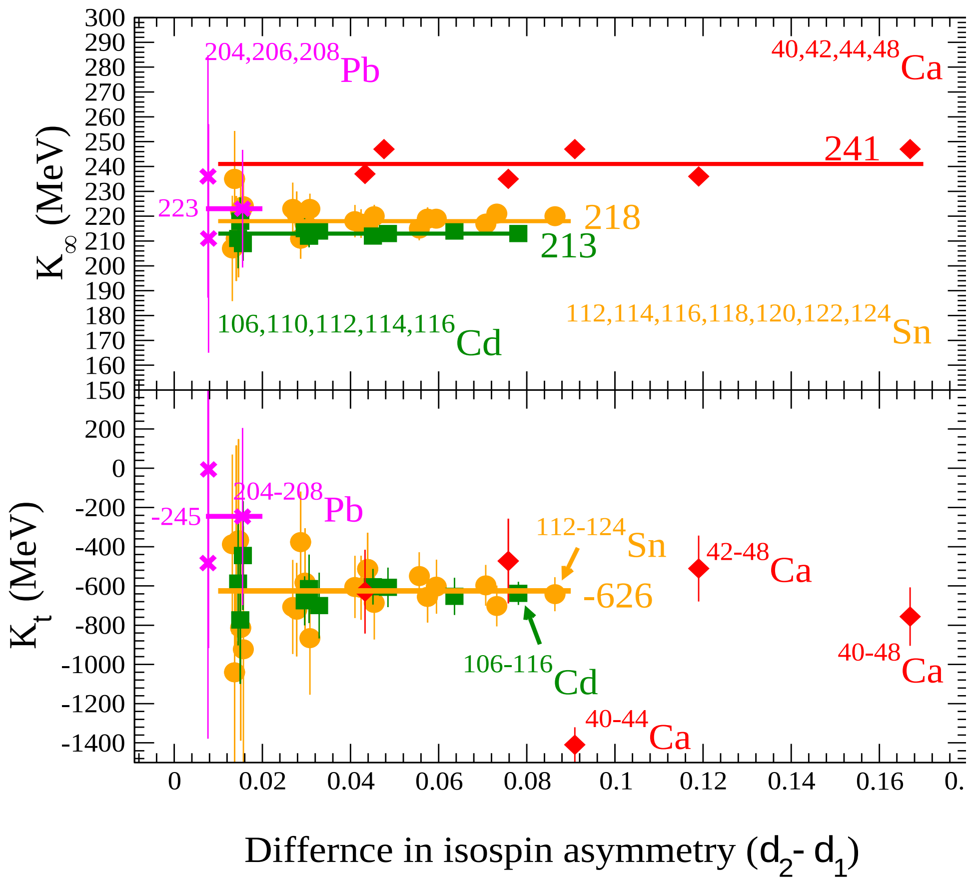

Nucleus	K_A (MeV)	Reference
^{40}Ca	144.46 ± 0.33	[17]
^{42}Ca	139.00 ± 1.09	
^{44}Ca	137.36 ± 0.66	
^{48}Ca	131.90 ± 4.13	
^{106}Cd	127.84 ± 0.86	[14]
^{110}Cd	124.59 ± 0.86	
^{112}Cd	123.59 ± 0.77	
^{114}Cd	120.95 ± 1.24	
^{116}Cd	118.96 ± 0.86	
^{112}Sn	131.86 ± 1.53	[12, 13]
^{114}Sn	129.45 ± 1.64	
^{116}Sn	127.11 ± 1.53	
^{118}Sn	126.39 ± 1.54	
^{120}Sn	125.45 ± 1.63	
^{122}Sn	121.33 ± 1.54	
^{124}Sn	120.17 ± 1.62	
^{204}Pb	136.93 ± 1.99	[15]
^{206}Pb	137.44 ± 1.99	
^{208}Pb	136.44 ± 1.99	

$K_\tau = -550$ MeV, RCNP

$K_\tau = +582$ MeV, TAMU

$K_\tau = -555 \pm 75$

$K_\tau = -550 \pm 100$

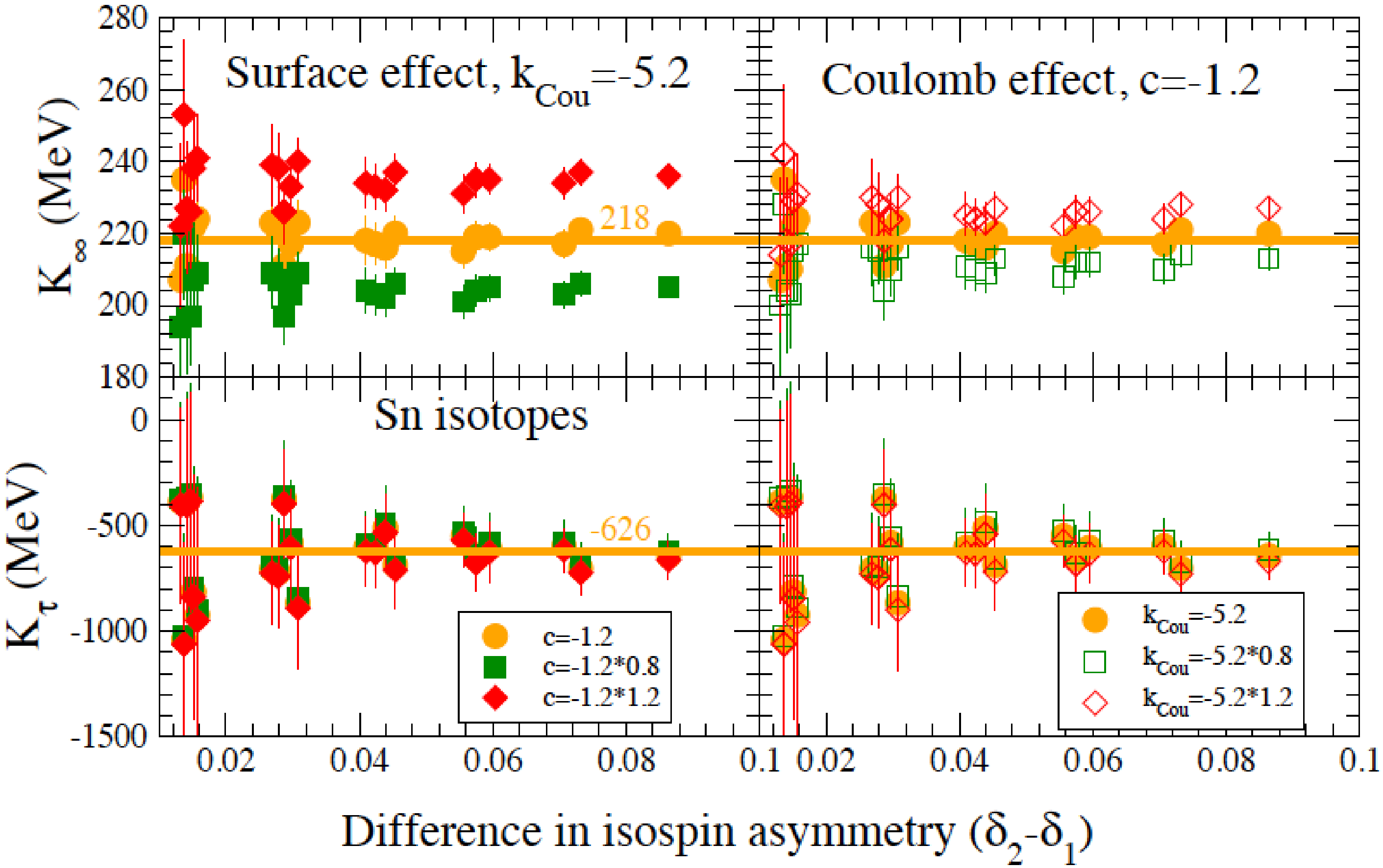

$$\sigma_{K_\tau} \approx \sqrt{\sigma^2_{K_{A_1}} + \sigma^2_{K_{A_2}}} \Big/ \left|\delta_1^2 - \delta_2^2\right|,$$

$$\sigma_{K_\infty} \approx \sqrt{(\delta_2^2 \cdot \sigma_{K_{A_1}})^2 + (\delta_1^2 \cdot \sigma_{K_{A_2}})^2} \Big/ \left|\delta_1^2 - \delta_2^2\right|$$

Bao-An Li and Wen-Jie Xie, Phys. Rev. C 104, 034610 (2021)

Fundamental physics underlying nuclear symmetry energy

Single-nucleon (Lane) potential in isospin-asymmetric matter: A. M. Lane, Nucl. Phys. 35, 676 (1962).

$$U_{n/p}(k,\rho,\delta) = U_0(k,\rho) \pm U_{sym1}(k,\rho)\bullet\delta + U_{sym2}(k,\rho)\bullet\delta^2 + o(\delta^3)$$

Hugenholtz-Van Hove (HVH) theorem:

N.M. Hugenholtz, L. Van Hove, Physica 24 (1958) 363.

$$E_F = \frac{d\xi}{d\rho} = \frac{d(\rho E)}{d\rho} = E + \rho\frac{dE}{d\rho} = E + P/\rho$$

$$E_{sym}(\rho) = \frac{1}{3}\frac{k_F^2}{2M} + \frac{1}{2}U_{sym,1}(\rho,k_F) + \frac{k_F}{6}\left(\frac{\partial U_0}{\partial k}\right)_{k_F} - \frac{1}{6}\frac{k_F^4}{2M^3}$$

S. Fritsch, N. Kaiser, W. Weise, Nuclear Phys. A 750 (2005) 259.

Using the K-matrix theory:

K.A. Brueckner, J. Dabrowski, Phys. Rev. B 134 (1964) 722.
J. Dabrowski, P. Haensel, Phys. Lett. B 42 (1972) 163;

$$E_{sym}(\rho) = \frac{1}{3}\frac{\hbar^2 k^2}{2m_0^*}|_{k_F} + \frac{1}{2}U_{sym,1}(\rho,k_F), \quad m_0^*(\rho,k) = \frac{m}{1+\frac{m}{\hbar^2 k}\frac{\partial U_0(\rho,k)}{\partial k}},$$

$$L(\rho) = \frac{2}{3}\frac{\hbar^2 k^2}{2m_0^*}|_{k_F} - \frac{1}{6}\left(\frac{\hbar^2 k^3}{m_0^{*2}}\frac{\partial m_0^*}{\partial k}\right)|_{k_F} + \frac{3}{2}U_{sym,1}(\rho,k_F) + \frac{\partial U_{sym,1}}{\partial k}|_{k_F}\cdot k_F + 3U_{sym,2}(\rho,k_F),$$

C. Xu, B.A. Li, L.W. Chen and C.M. Ko, NPA 865, 1 (2011)

$$m_{n-p}^* \approx 2\delta\frac{m}{\hbar^2 k_F}\left[-\frac{dU_{sym,1}}{dk} - \frac{k_F}{3}\frac{d^2U_0}{dk^2} + \frac{1}{3}\frac{dU_0}{dk}\right]_{k_F}\left(\frac{m_0^*}{m}\right)^2$$

Bao-An Li, Bao-Jun Cai, Lie-Wen Chen and Jun Xu,
Progress in Particle and Nuclear Physics 99 (2018) 29–119

Density and momentum dependence of Isoscalar and Isovector potentials
Gogny Hartree-Fock predictions using 11 popular Gogny (finite-range) forces

PHYSICAL REVIEW C 90, 054327 (2014)

Isovector properties of the Gogny interaction

Roshan Sellahewa and Arnau Rios

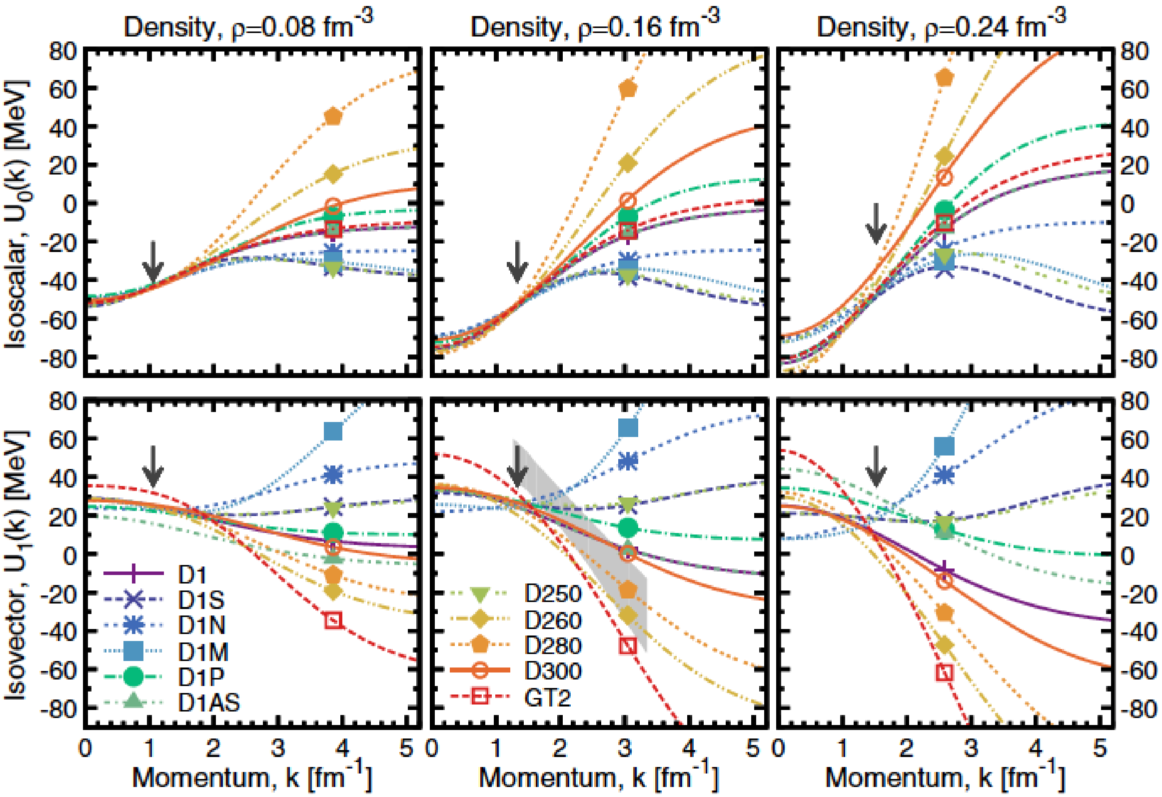

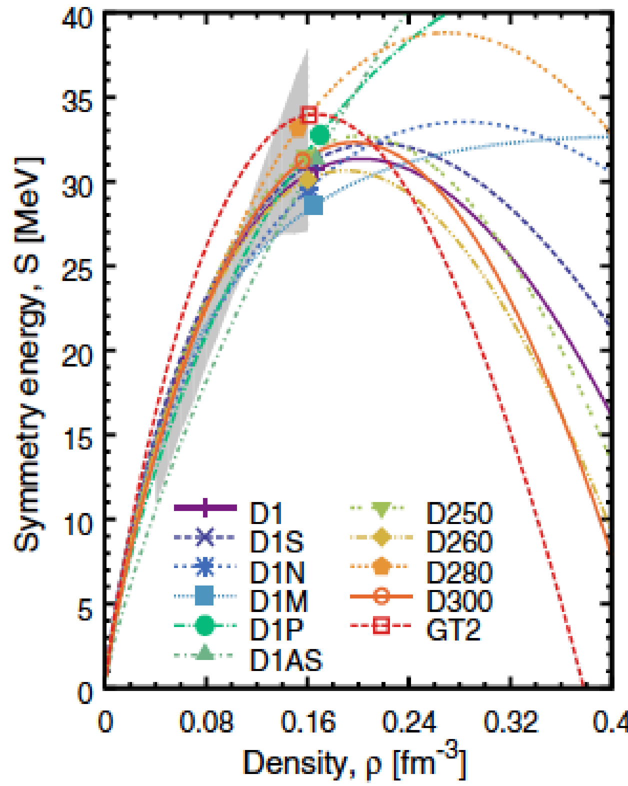

Momentum dependence of the nucleon optical potential at normal density

X.H. Li, W.J. Guo, B.A. Li, L.W. Chen, F.J. Fattoyev and W.G. Newton PLB 743 (2015) 408

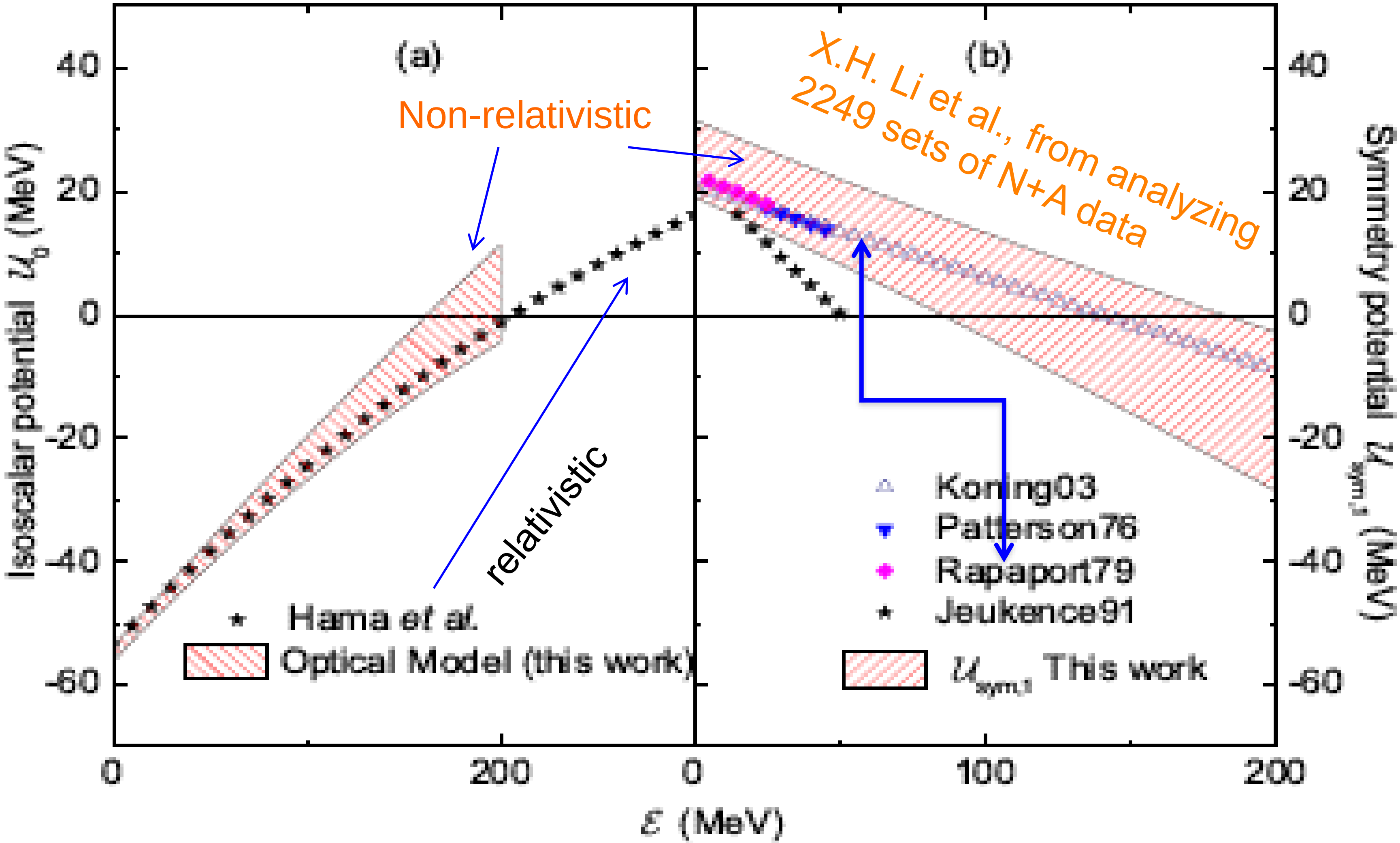

Definitions of nucleon effective masses

J.P. Jeukenne, A. Lejeune and C. Mahaux
Physics Reports, 25, 83 (1976)

The nucleon k-mass: $$\frac{M_J^{*,k}}{M} = \left[1 + \frac{M}{k}\frac{\partial U_J}{\partial k}\right]^{-1}$$

The nucleon E-mass: $$\frac{M_J^{*,E}}{M} = 1 - \frac{\partial U_J}{\partial E}$$

The total effective mass is given equivalently in any of the following 2 definitions

given the on-mass shell dispersion relation: $E_J = k^2/2M + U_J(\rho, \delta, k, E)$

$$\frac{M_J^*}{M} = 1 - \left.\frac{dU_J(\rho, \delta, k(E), E)}{dE}\right|_{E(k_F^J)} = \left[1 + \frac{M}{k_F^J}\left.\frac{dU_J(\rho, \delta, k, E(k))}{dk}\right|_{k_F^J}\right]^{-1}$$

The total effective mass = E-mass × k-mass: $$\frac{M_J^*}{M} = \frac{M_J^{*,E}}{M} \cdot \frac{M_J^{*,k}}{M}$$

Brueckner Hartree-Fock and Relativistic Hartree-Fock predictions

A. Li, J.N. Hu, X.L. Shang, W. Zuo, Phys. Rev. C 93 (2016) 015803.

Total effective mass K-effective mass E-effective mass

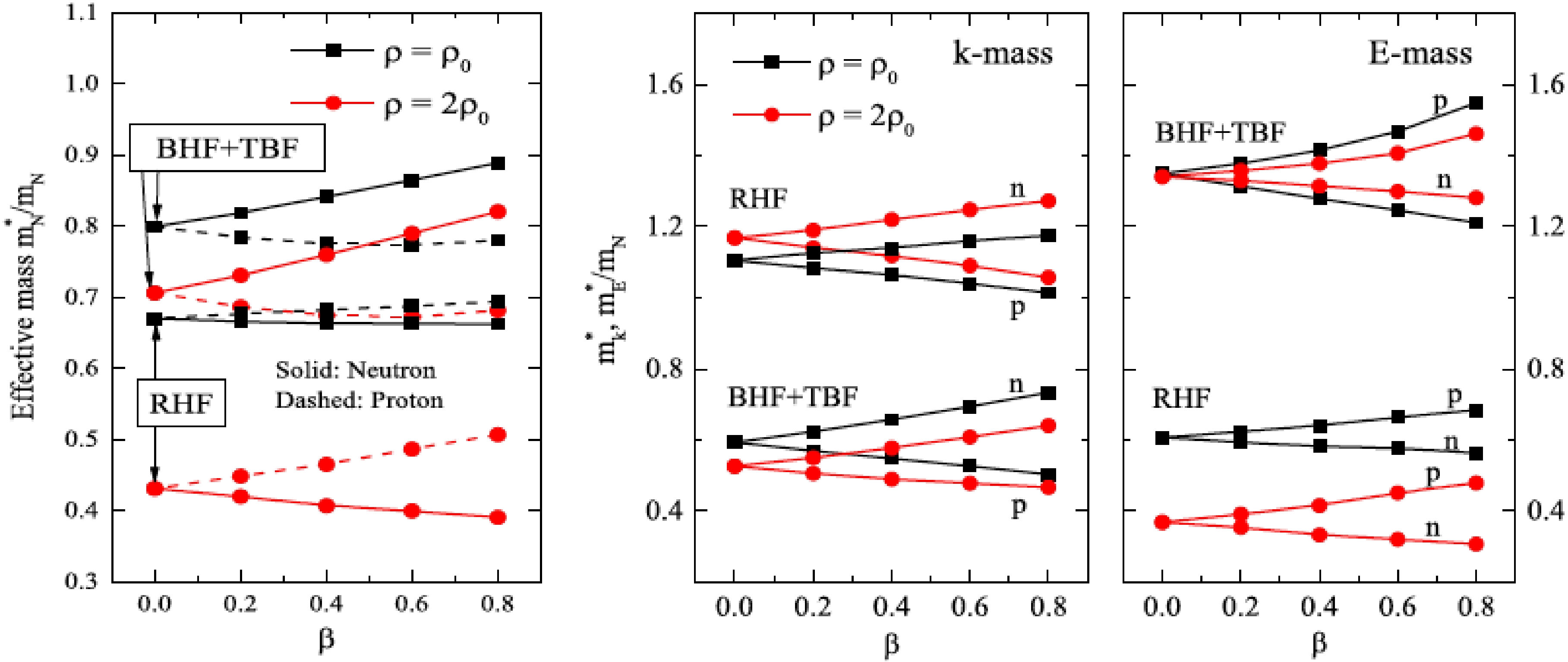

They have different and model-dependent neutron-proton effective mass splitings

Neutron-proton total effective mass splitting from optical potentials

In primordial nucleosynthesis: $(n/p)_{eq} = e^{-m^*_{n-p}/T}$

$$m^*_{n-p}(\rho_0,\delta) \equiv \frac{m^*_n - m^*_p}{m} = \left.\frac{\frac{m}{\hbar^2 k_F}(dU_p/dk - dU_n/dk)}{(1+\frac{m}{\hbar^2 k_F}dU_p/dk)(1+\frac{m}{\hbar^2 k_F}dU_n/dk)}\right|_{k_F}$$

$$m^*_{n-p}(\rho_0,\delta) \approx \delta \cdot \left[3E_{\rm sym}(\rho_0) - L(\rho_0) - \frac{1}{3}\frac{m}{m^*_0}E_F(\rho_0)\right] \Big/ \left[E_F(\rho_0)\cdot(m/m^*_0)^2\right]$$

Bao-An Li and Xiao Han, **PLB727 (2013) 276**

a positive value for the $m^*_{n-p}(\rho_0,\delta)$ requires that $L(\rho_0) \leq 76$

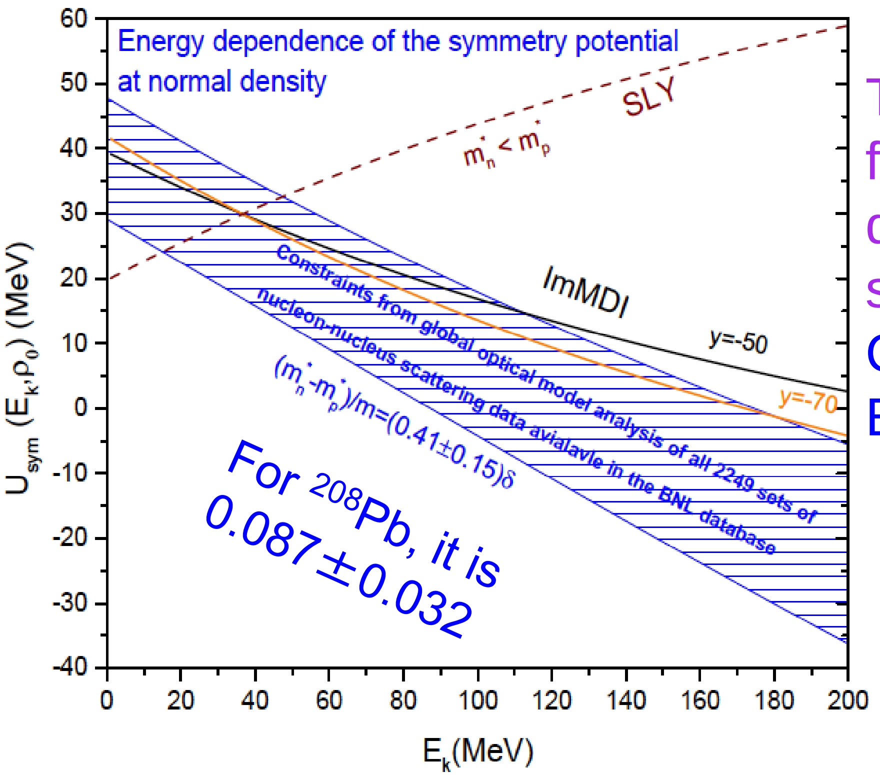

The proton-neutron effective mass splitting for ^{208}Pb is **+0.054** at its center from dispersive optical model analysis of n+Pb scatterings

Charity, Dickhoff, Sobotka and Waldecker EPJA 50, 3 (2014) 64

What we know about the neutron-proton total effective mass splitting

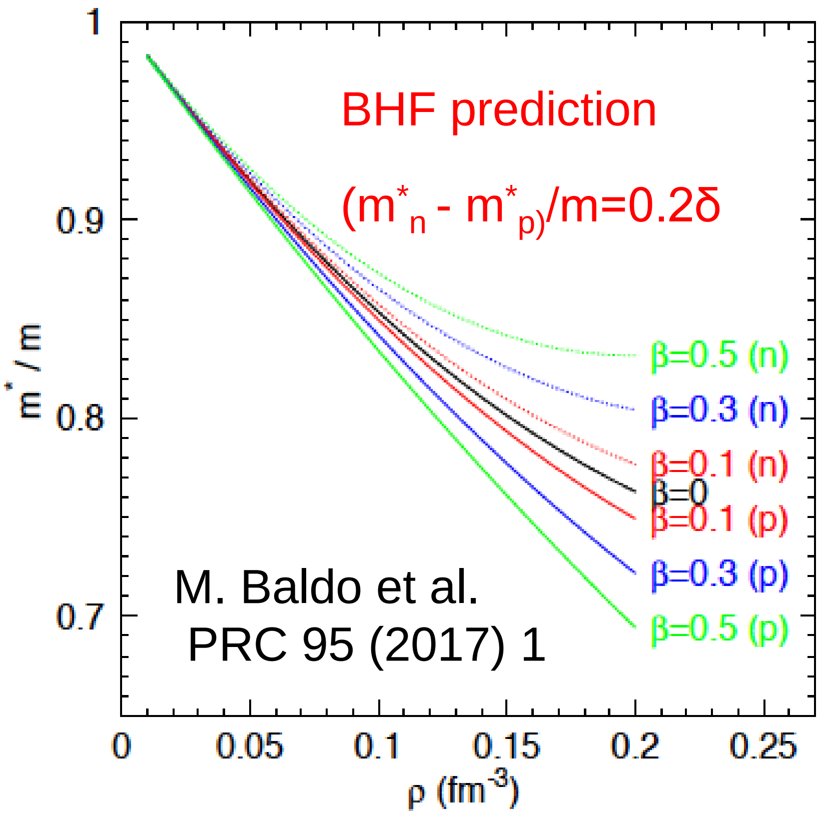

Extracting the $m^*_n - m^*_p$ from experiments

(1) Optical model analysis

C. Xu et al. 2010,

$$(m_n^* - m_p^*)/m = (0.32 \pm 0.15)\delta$$

B. Charity 2010

$(m^*_n - m^*_{p})/m=0.26\delta$

X. H. Li, 2014

$$m^*_{n-p} = (0.41 \pm 0.15)\delta$$

(2) Systematics of symmetry energy

B.A. Li and X. Han, 2013

$$m^*_{n-p} = (0.27 \pm 0.25)\delta$$

(3) Dipole polarizability of Pb

Z. Zhang and L.W. Chen, 2016

$(m^*_n - m^*_{p})/m=(0.27\pm0.15)\delta$

(4) n/p ratio in Sn+Sn reactions at 120 MeV/A

P. Morfouace et al., PLB 799 (2019) 135045

$$\Delta m^*_{np} = (m_n^* - m_p^*)/m_N = -0.05^{+0.09}_{-0.09}\delta.$$

Density dependence of the neutron-proton effective mass splitting from chiral EFT
T.R. Whitehead et al. (2021)

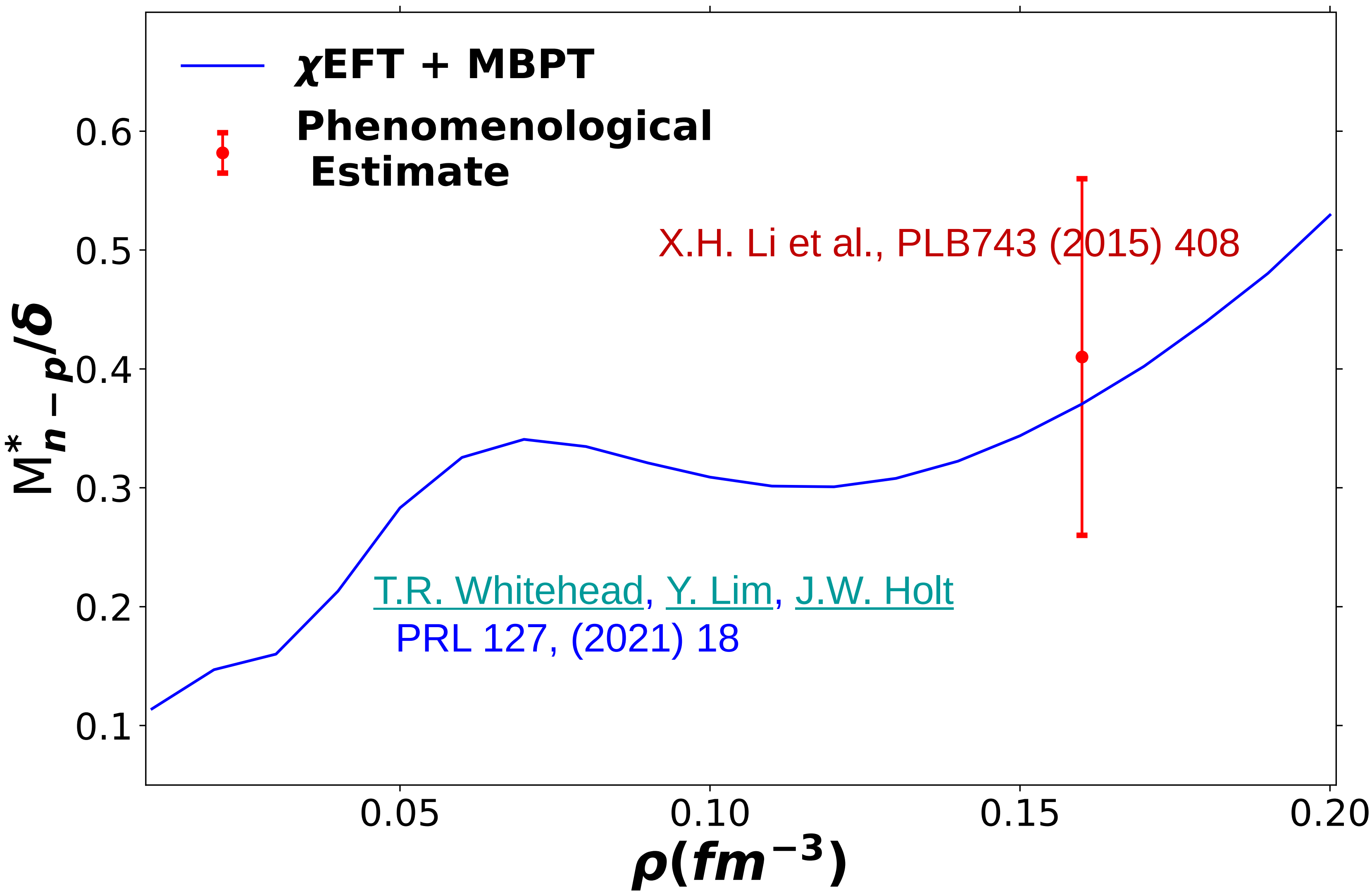

Constraining the nucleon effective E-mass

$$\frac{M_J^{*,\mathrm{E}}}{M} = 1 - \frac{\partial U_J}{\partial E}$$

Using the Migdal (1957)-Luttinger (1960) Theorem:

(occupation renormalization function)

A.B. Migdal, Sov. Phys. JEPT. 5 (1957) 333.

J.M. Luttinger, Phys. Rev. 119 (1960) 1153.

$$Z_{\mathrm{F}}^{J} = n^{J}_{k_{\mathrm{F}}^{J}-0} - n^{J}_{k_{\mathrm{F}}^{J}+0} = M / M_{\mathrm{E}}^{J,*}$$

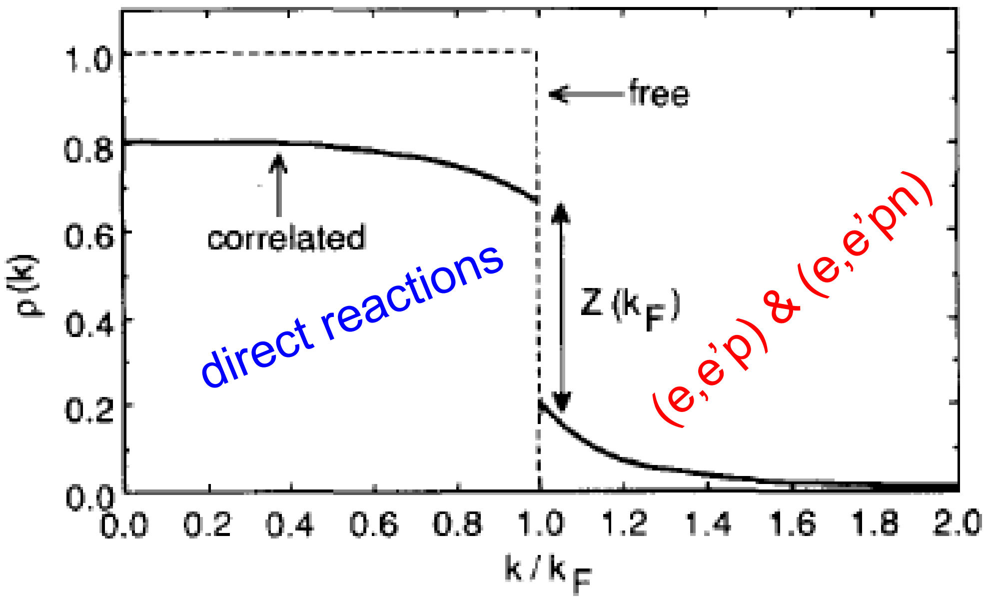

C. MAHAUX and R. SARTOR

Physics Reports 211, 53 (1992).

Example: (1) get the total effective mass from optical potentials,
(2) get the E-mass using the Migdal-Luttinger theorem from the n(k) constrained by SRC data of e-A reaction
(3) then get the k-mass from the relation $\frac{M_J^*}{M} = \frac{M_J^{*,\mathrm{E}}}{M} \cdot \frac{M_J^{*,\mathrm{k}}}{M}$

Protons are more energetic and more correlated in neutron-rich matter

Short-Range Correlation in asymmetric matter

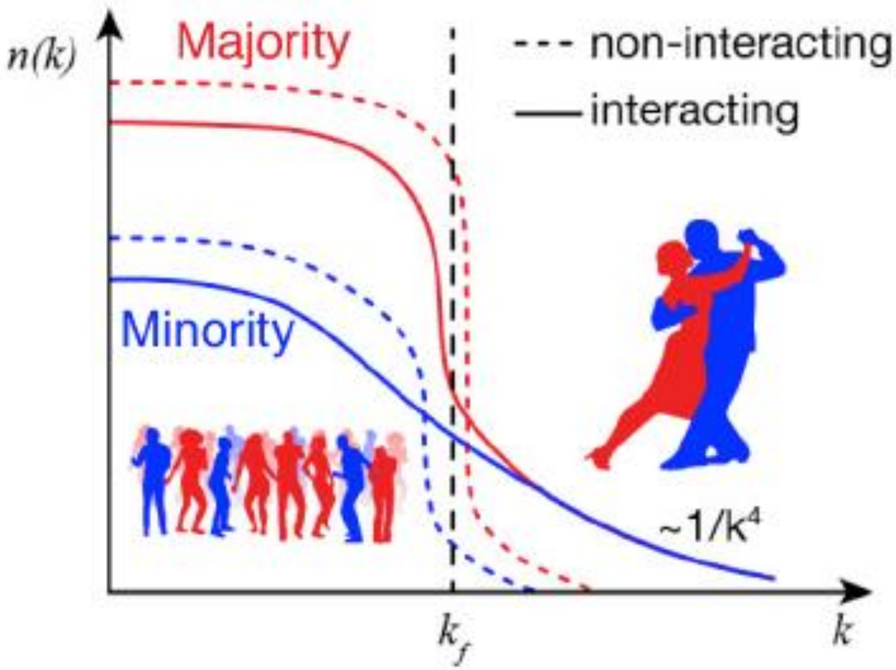

O. Hen et al.,
Science 346, 614 (2014)

Average depletion of the Fermi sea
For neutrons and protons based on
the available SRC-data

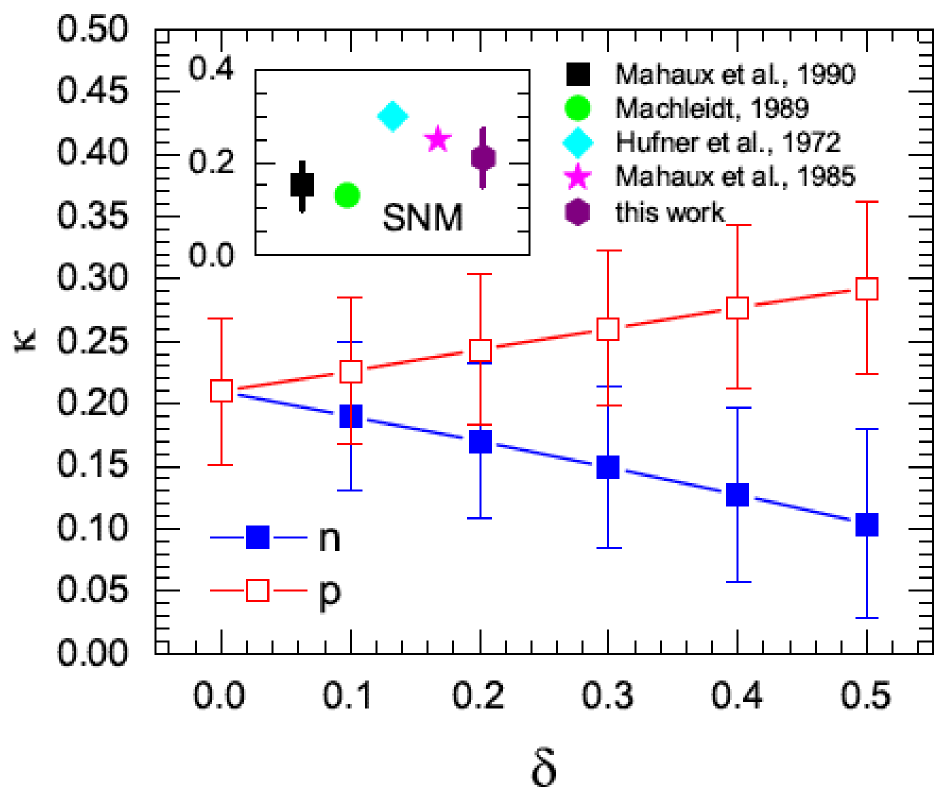

B.J. Cai, B.A. Li, Phys. Lett. B 757 (2016) 79.

The Jlab finding is consistent with earlier findings from the spectroscopic factors of direction reactions and the dispersive optical model analysis of p+nucleus scattering

The minority component is more correlated!

Example I: proton occupation from p+^{40}Ca, p+^{48}Ca, and p+^{60}Ca (prediction)

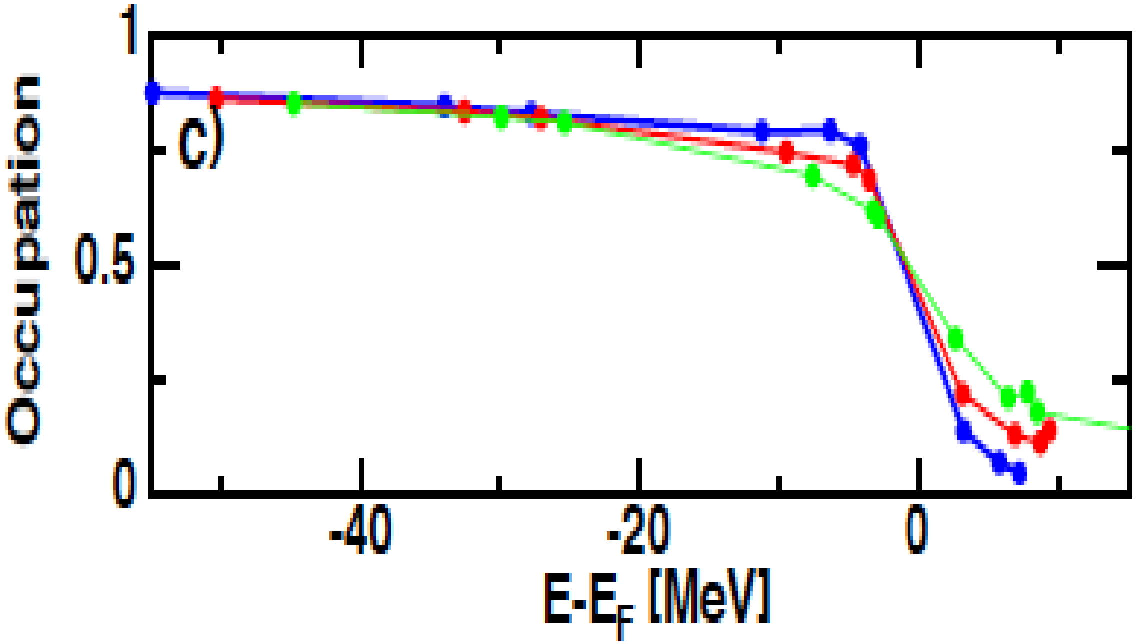

PRL 97, 162503 (2006)

Asymmetry dependence of proton correlations.

R. J. Charity[1], L. G. Sobotka[1,2], W. H. Dickhoff[2]

Constraining the nucleon effective E-mass

$$\frac{M_J^{*,\mathrm{E}}}{M} = 1 - \frac{\partial U_J}{\partial E}$$

$$\mathrm{Z}_{\mathrm{F}}^{J} = n^{J}_{k_{\mathrm{F}}^{J}-0} - n^{J}_{k_{\mathrm{F}}^{J}+0} = M/M_{\mathrm{E}}^{J,*}$$

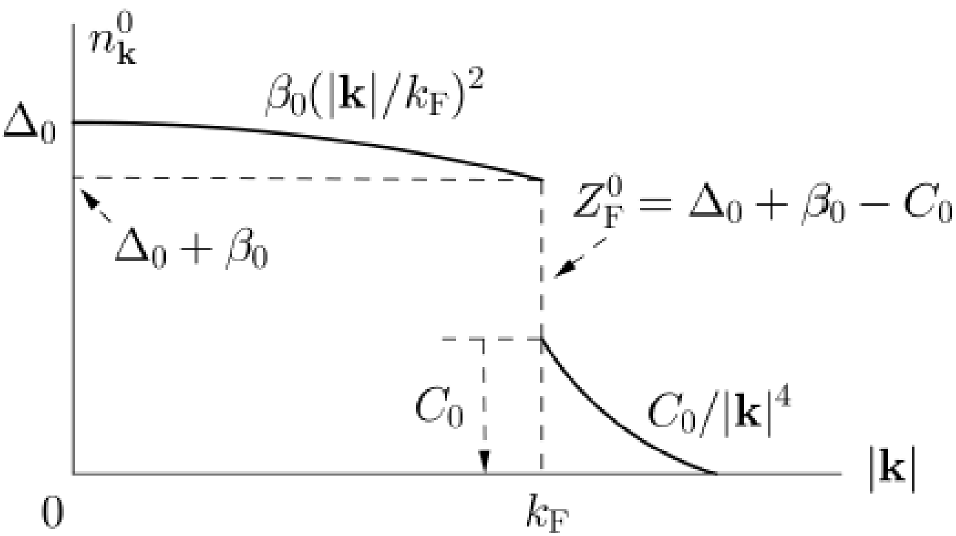

In symmetric nuclear matter based on available SRC data

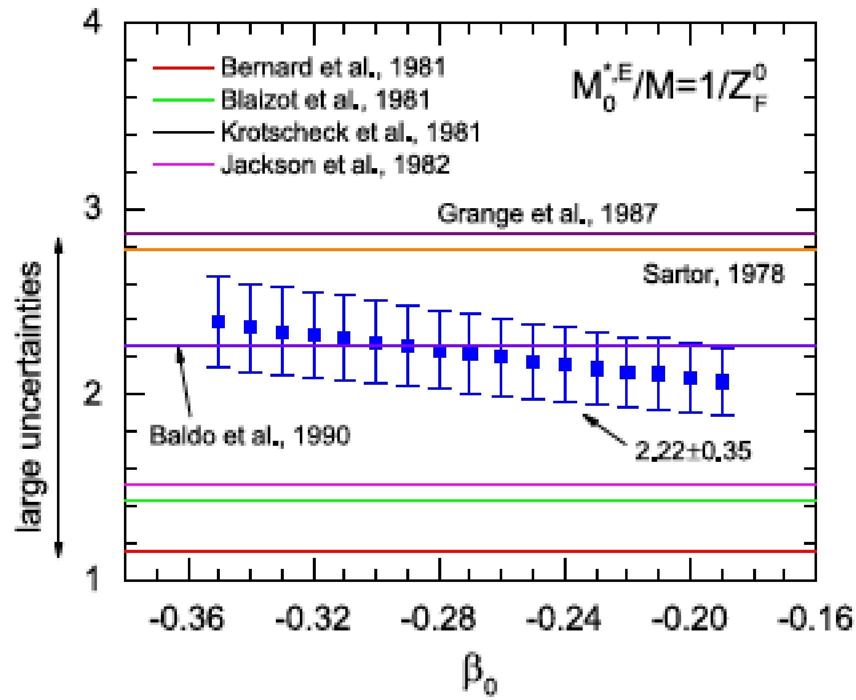

Bao-Jun Cai and Bao-An Li
PLB 757, 79 (2016)

Isospin fractionation during heavy-ion reactions

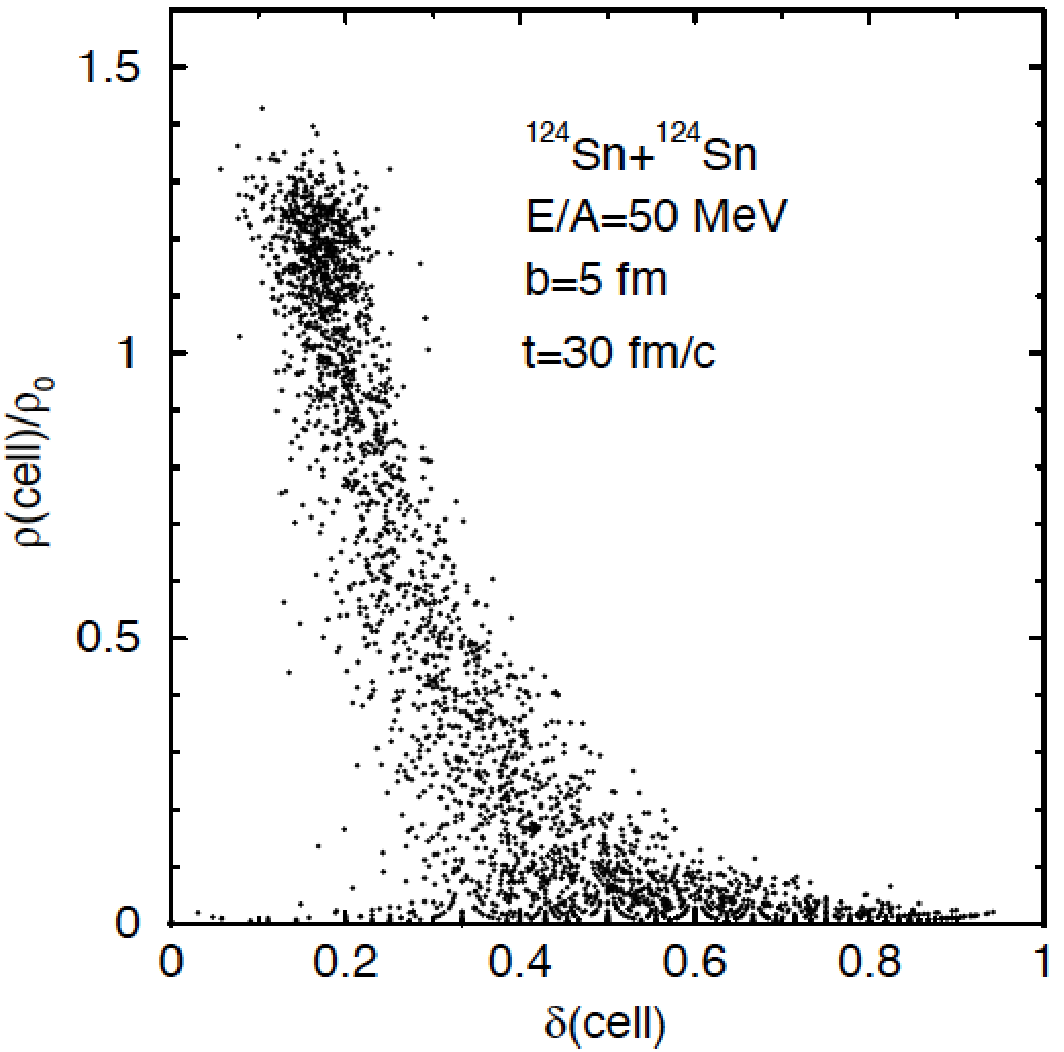

Bao-An Li, Andrew T. Sustich, Bin Zhang, PRC 64, 054604 (2001)

Effects of symmetry energy on isospin fractionation

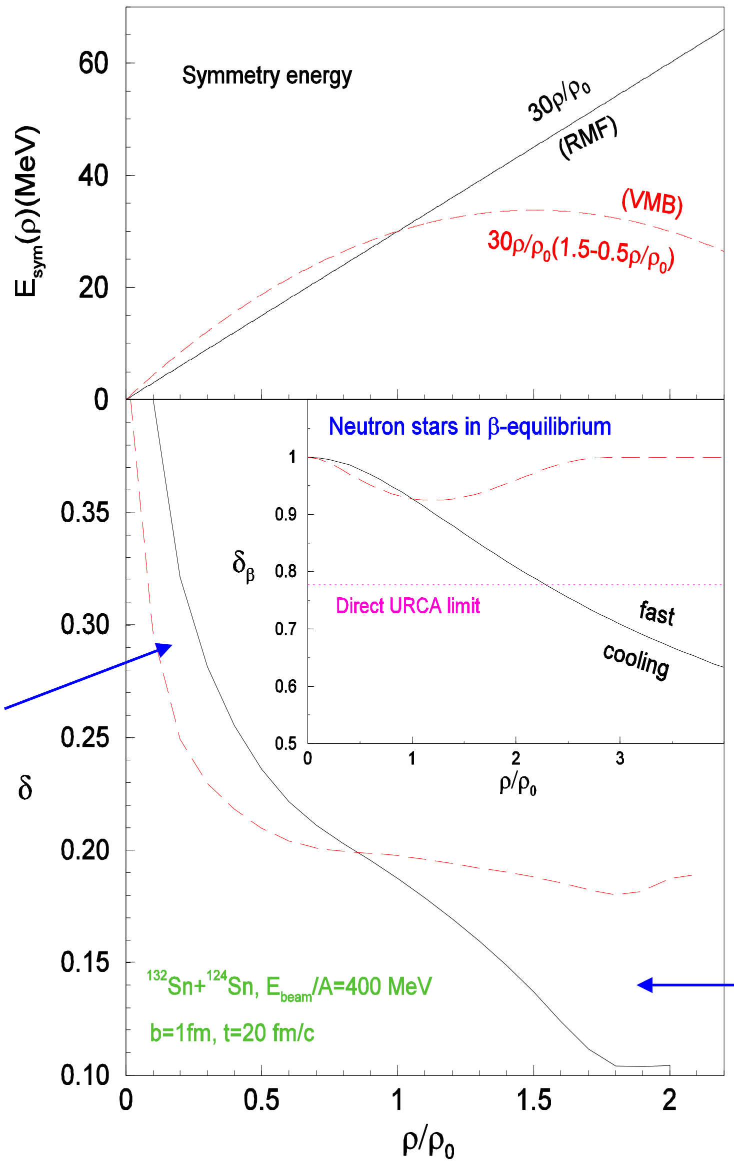

$$E(\rho,\delta) = E(\rho,0) + E_{sym}(\rho)\delta^2$$

high density region is more neutron-rich with soft symmetry energy

n/p spectrum ratio of pre-equilibrium emission probing neutron-proton effective mass splitting

The density dependence of isospin asymmetry in neutron stars and heavy-ion reactions are similar

π^-/π^+ ratio at freeze-out and neutron-proton differential flow probing high-density E_{sym}

Bao-An Li, Phys. Rev. Lett. 88 (2002) 192701

Evolution of nucleon total effective masses and in-medium NN Xsections

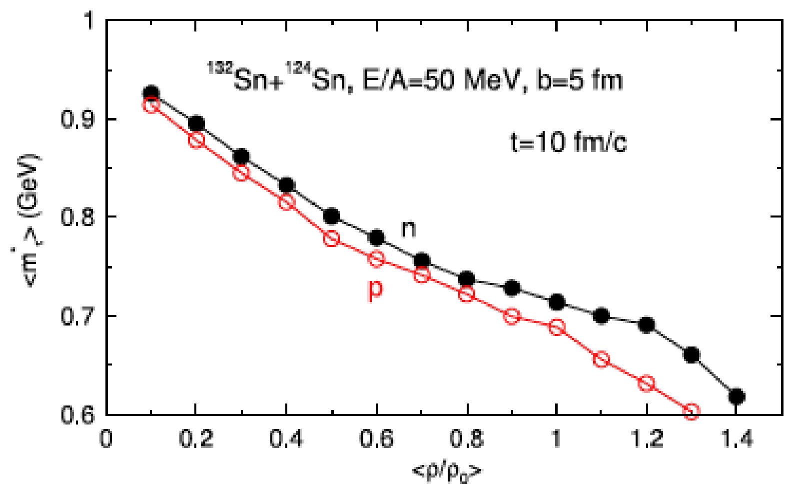

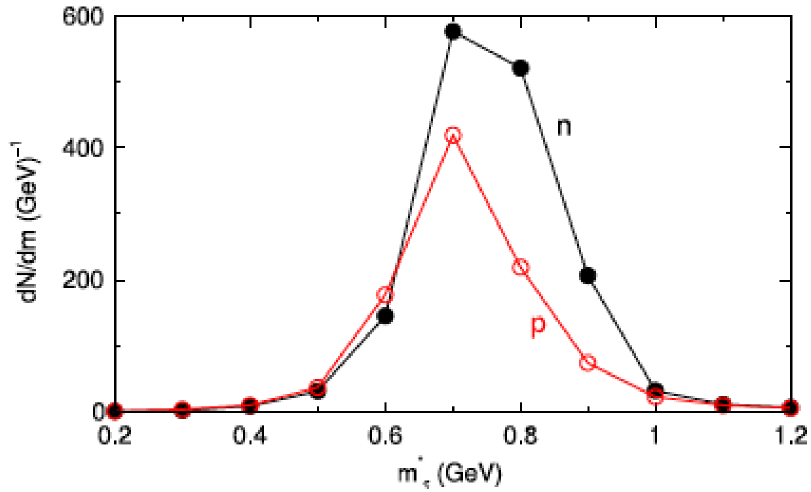

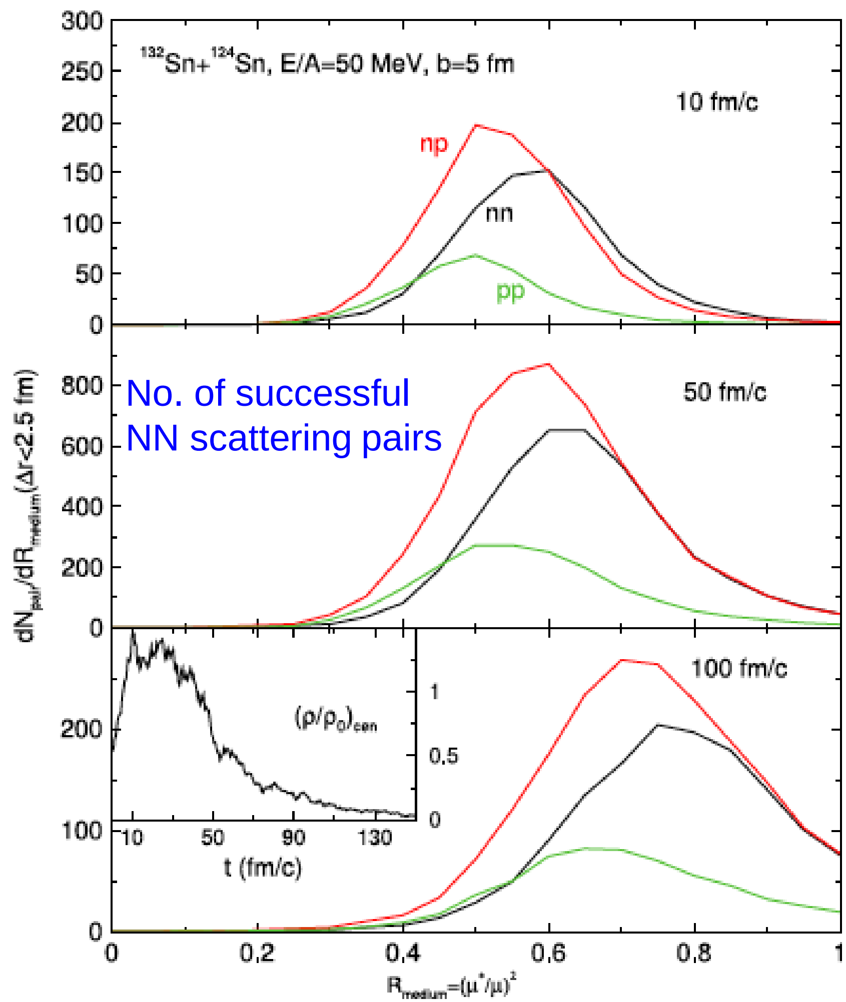

Bao-An Li and Lie-Wen Chen, Phys. Rev. C72, 064611 (2005).

Reduction of in-medium Xsection

$$\sigma_{medium} / \sigma_{free} \approx \left(\frac{\mu^*_{NN}}{\mu_{NN}} \right)^2$$

μ^*_{NN} is the reduced effective mass of the colliding nucleon pair NN

Isospin dependence of nucleon mean free path

$\lambda_p^{-1} = \rho_p\sigma_{pp}^* + \rho_n\sigma_{pn}^*$ and $\lambda_n^{-1} = \rho_n\sigma_{nn}^* + \rho_p\sigma_{np}^*$

$$\lambda_J = \frac{k_R^J}{2M_J^{*,k}|W_J|}$$

Real part of the nucleon momentum

K-mass

Imaginary part of the single-nucleon potential

J.W. Negele and K. Yazaki, PRL 47, 71 (1981)

$$E = k^2/2m + \Sigma(k, E) . \quad (1)$$

The self-energy is in general complex, and it will be useful to write

$$\Sigma(k, E) \equiv U(k, E) + i\, W(k, E) , \quad (2)$$

$$k \equiv k_R + ik_I , \quad (3)$$

and the imaginary part yields the mean free path

$$k_I = 1/2\lambda . \quad (4)$$

Nucleon mean free path in neutron-rich matter:

$$\lambda_J \approx \lambda_0 + \lambda_{sym}\tau_3^J\delta$$

+1 for neutrons
-1 for protons

Isoscalar isovector

PHYSICAL REVIEW C 93, 064603 (2016)

Microscopic optical potential for exotic isotopes from chiral effective field theory

J. W. Holt,[1,2] N. Kaiser,[3] and G. A. Miller[1]

(their optical potentials = minus the optical potentials by others in this talk)

$$W_J \approx W_0 + W_{sym}\tau_3^J\delta$$

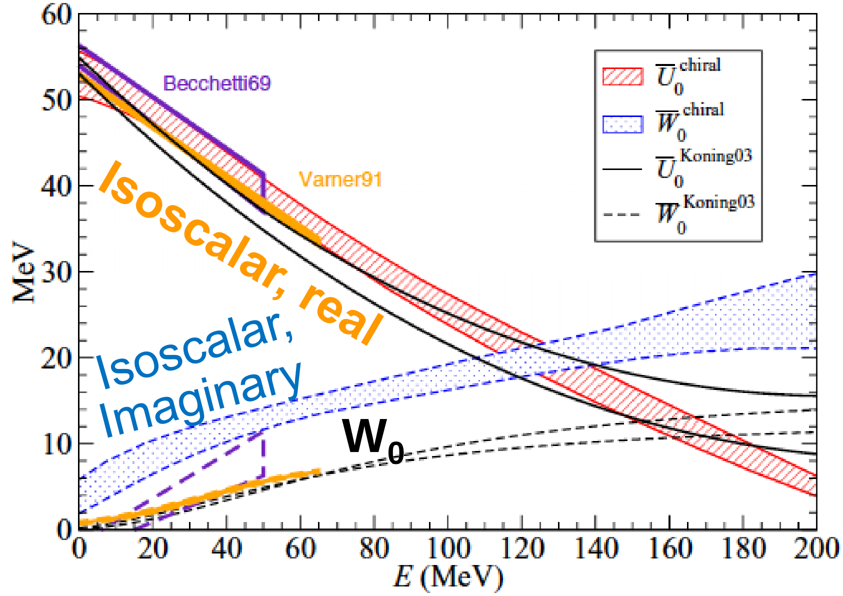

FIG. 1. Energy dependence of the real and imaginary parts of the microscopic optical potential from chiral two- and three-body forces for symmetric nuclear matter at saturation density ρ_0. Shown for comparison are the global phenomenological potentials of Refs. [19–21].

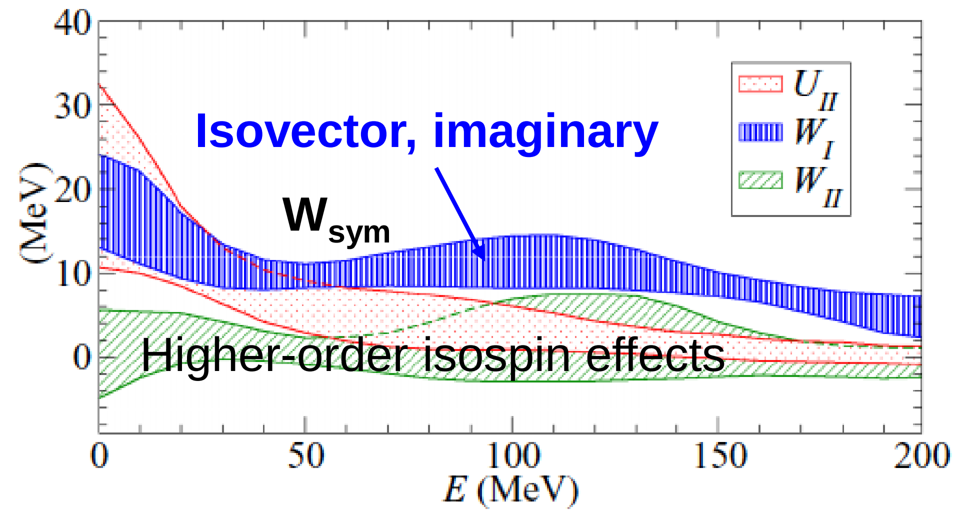

FIG. 6. Energy dependence of the isovector imaginary optical potential at saturation density from chiral two- and three-body forces. Also shown are the subleading δ_{np}^2 contributions to both the real and imaginary potentials.

Isospin dependence of nucleon mean free path in neutron-rich matter

PHYSICAL REVIEW C **90**, 064602 (2014)

In-medium effects for nuclear matter in the Fermi-energy domain

O. Lopez,[1] D. Durand,[1] G. Lehaut,[1] B. Borderie,[2] J. D. Frankland,[3] M. F. Rivet,[2] R. Bougault,[1] A. Chbihi,[3] E. Galichet,[2,4] D. Guinet,[5] M. La Commara,[6] N. Le Neindre,[1] I. Lombardo,[6] L. Manduci,[7] P. Marini,[3,8] P. Napolitani,[2] M. Pârlog,[1] E. Rosato,[6] G. Spadaccini,[6] E. Vient,[1] and M. Vigilante[6]

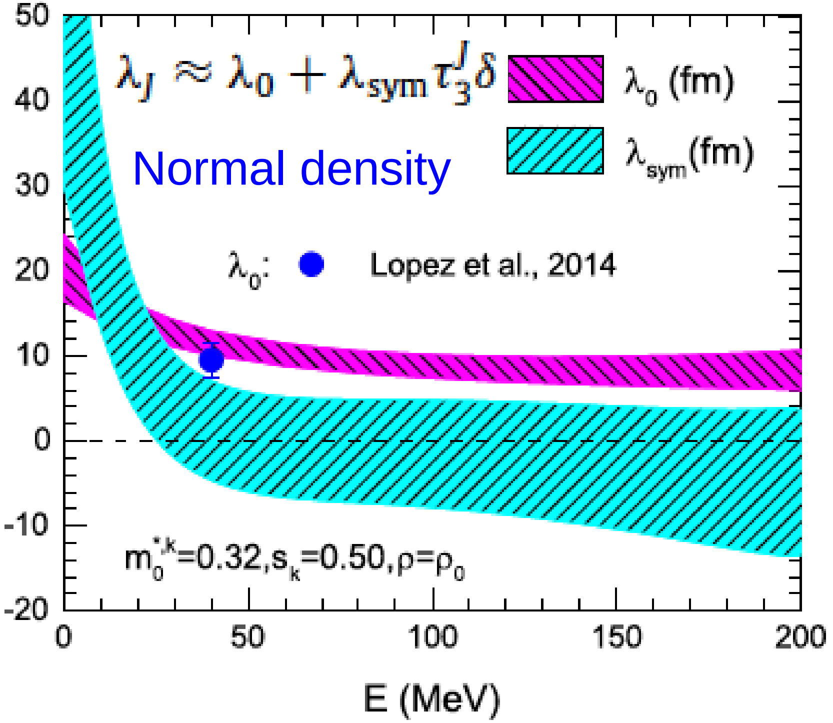

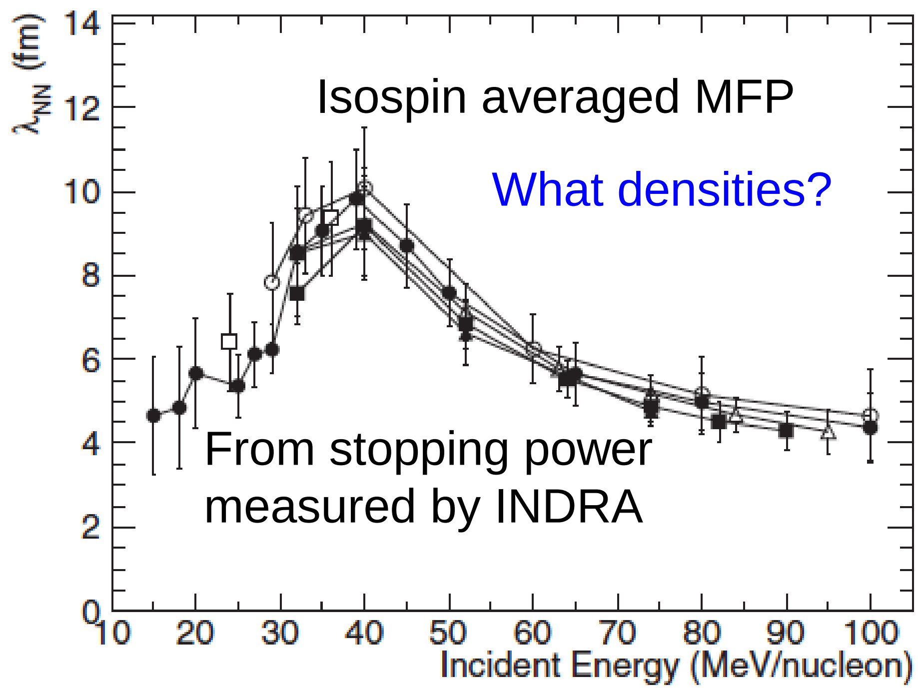

(1) the calculated isoscalar MFP is too long w.r.t. the INDRA finding, opposite trends at low E

(2) neutrons have much longer MFP than protons at low energies

B.-A. Li et al. / Progress in Particle and Nuclear Physics 99 (2018) 29–119

Constraints on L as of 2013 based on 29 analyses of data

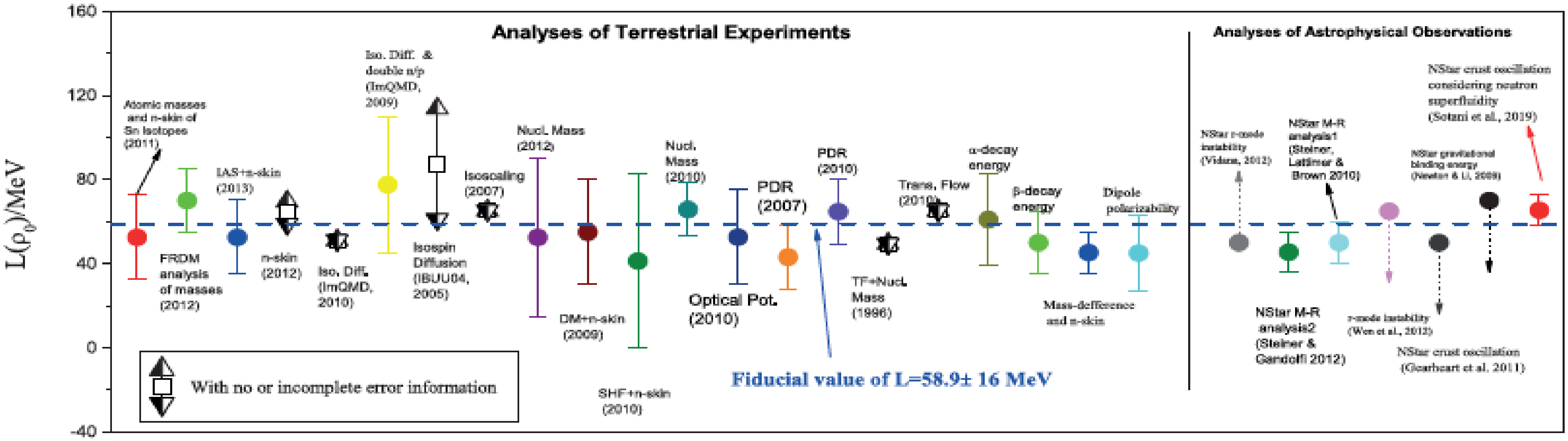

Bao-An Li and Xiao Han, **Phys. Lett. B727 (2013) 276**

L=58.7±28.1 MeV

Fiducial value as of 2016 from surveying 53 analyses

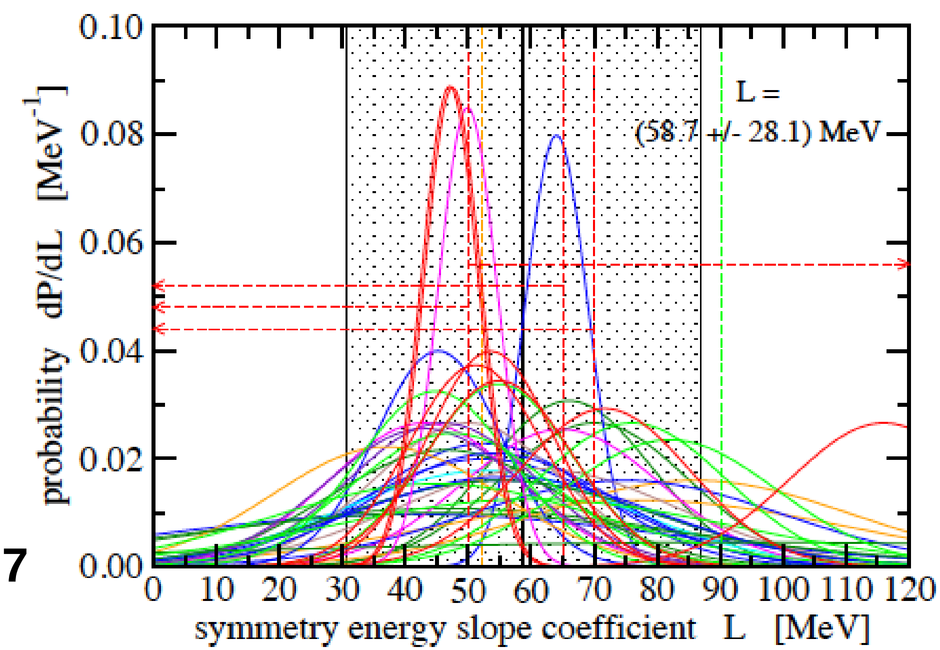

M. Oertel, M. Hempel, T. Klähn, S. Typel

Review of Modern Physics 89 (2017) 015007

Progress in Constraining Nuclear Symmetry Energy Using Neutron Star Observables Since GW170817 by the community

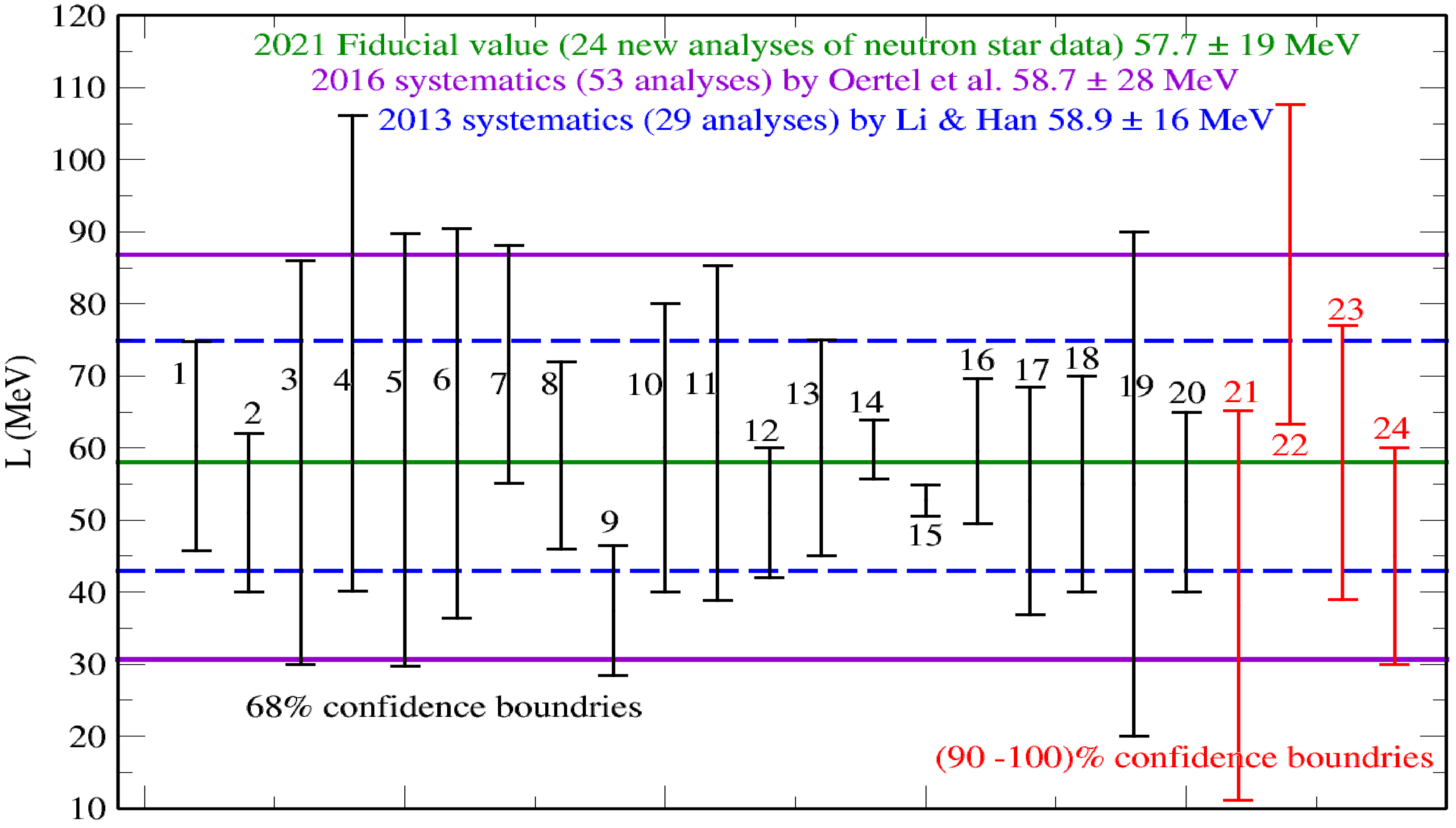

Curvature K_{sym} of the symmetry energy at saturation density

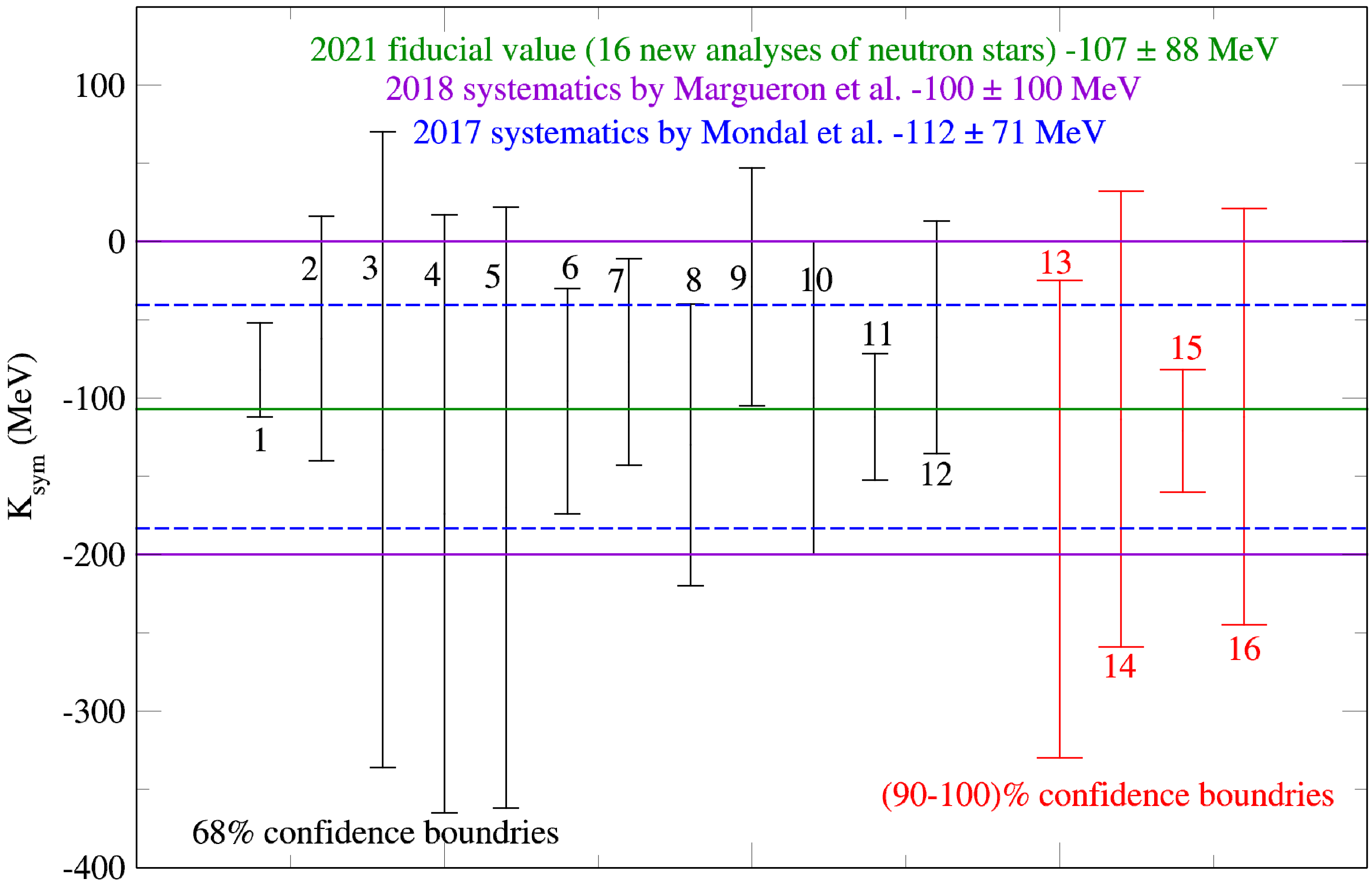

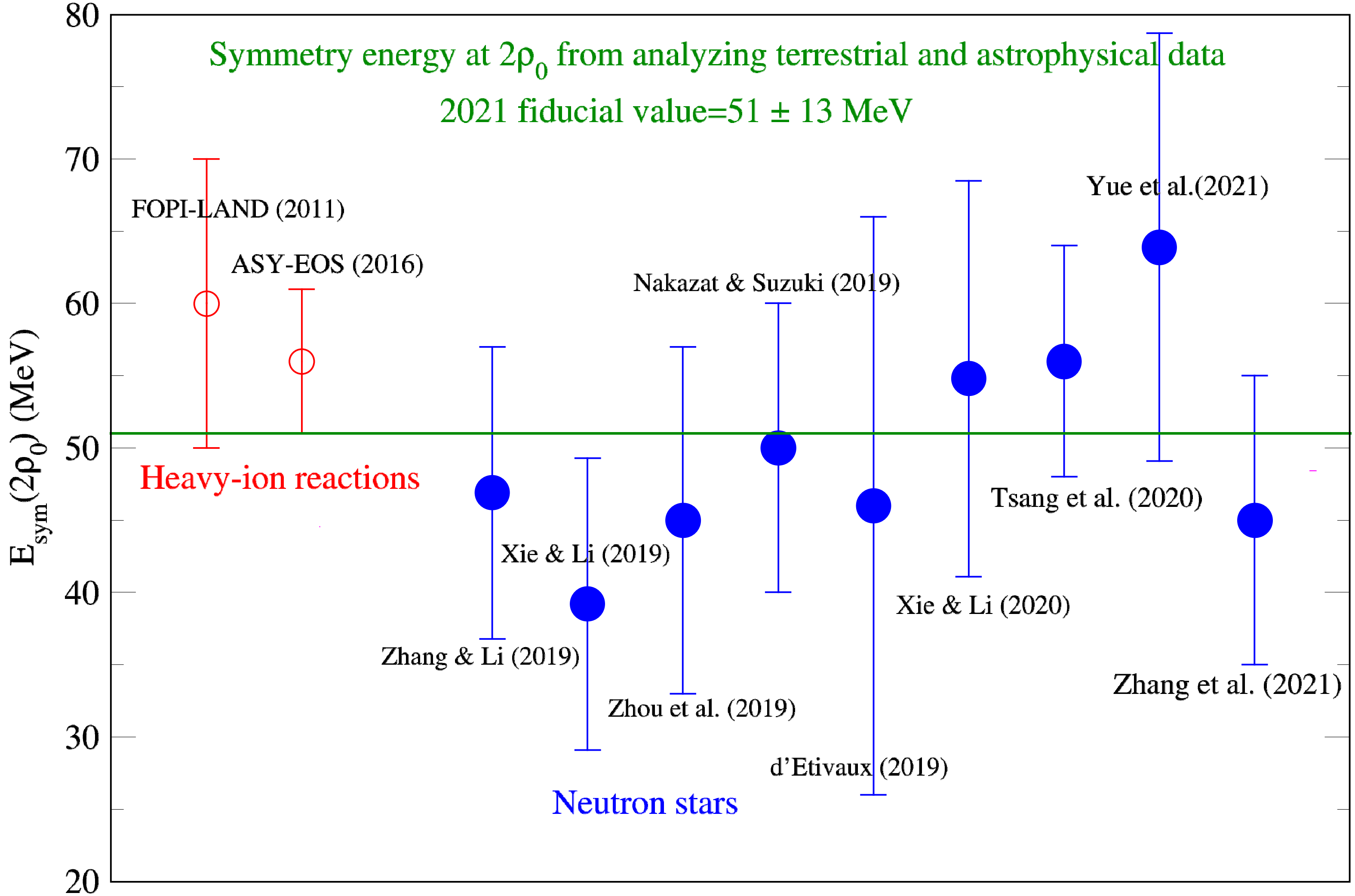

Symmetry energy at 2ρ0 from analyzing terrestrial and astrophysical data
2021 fiducial value=51 ± 13 MeV
FOPI-LAND (2011)
ASY-EOS (2016)
Heavy-ion reactions
Nakazat & Suzuki (2019)
Yue et al.(2021)
Tsang et al. (2020)
Xie & Li (2019)
Zhang & Li (2019)
Zhou et al. (2019)
d'Etivaux (2019)
Xie & Li (2020)
Zhang et al. (2021)
Neutron stars
Esym(2ρ0) (MeV)
80
70
60
50
40
30
20

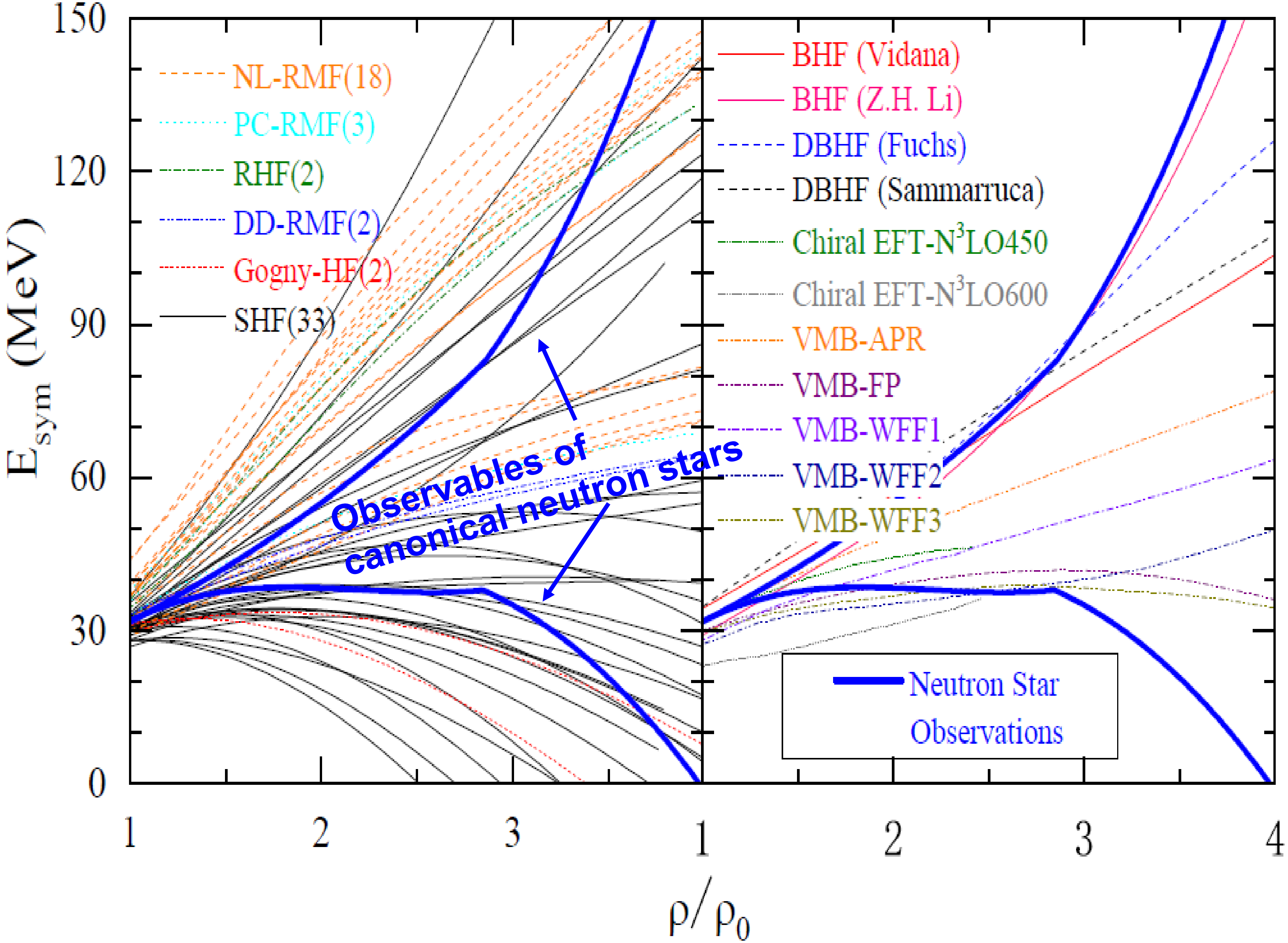

B.A. Li, P.G. Krastev, D.H. Wen and N.B. Zhang, Eur. Phys. J. A (2019) 55: 117

THE ASTROPHYSICAL JOURNAL, 921:111 (11pp), 2021 November 10

https://doi.org/10.3847/1538-4357/ac1e8c

Impact of NICER's Radius Measurement of PSR J0740+6620 on Nuclear Symmetry Energy at Suprasaturation Densities

Nai-Bo Zhang[1] and Bao-An Li[2]

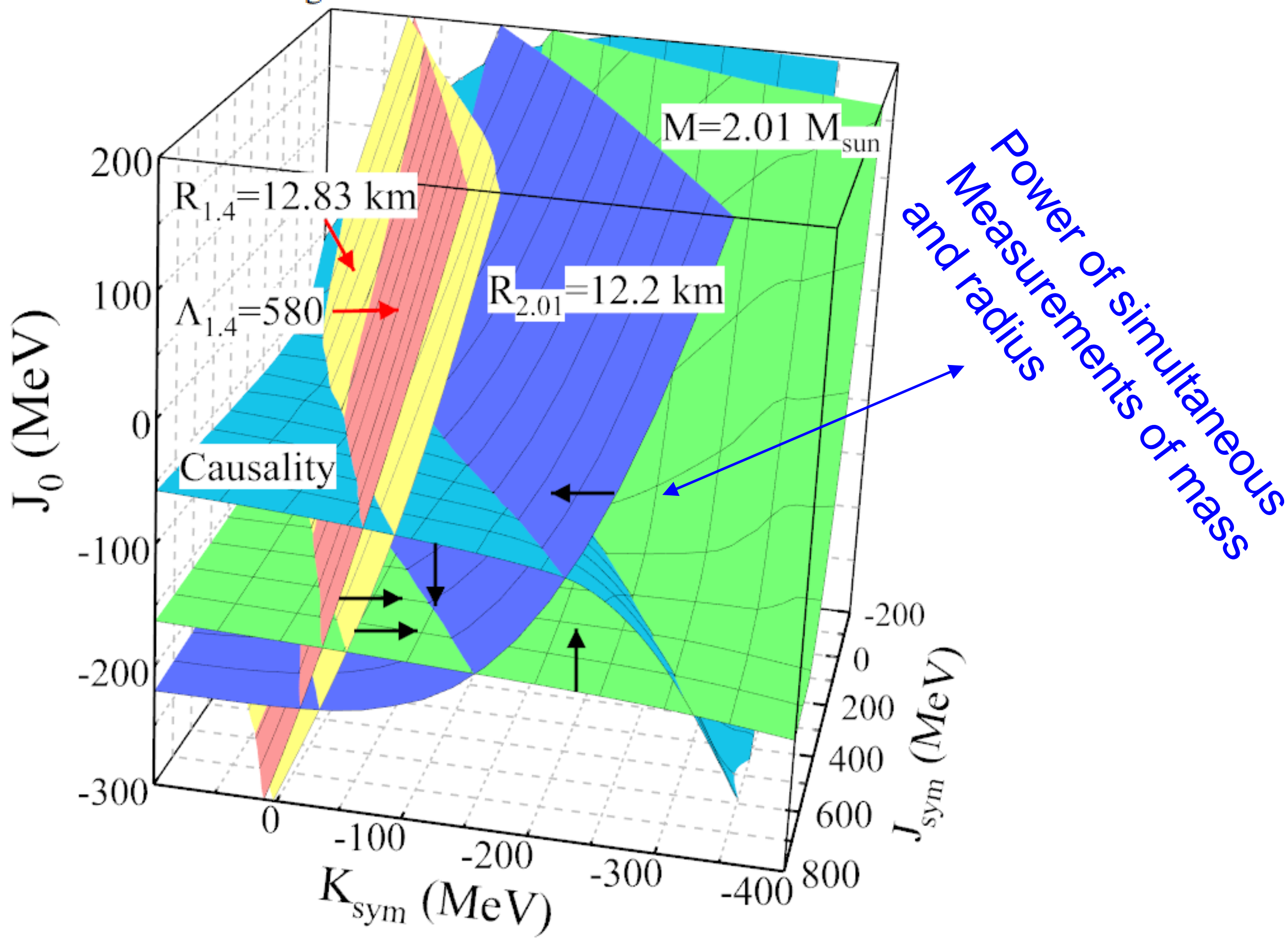

NICER results :

Mass: $2.08 \pm 0.07\, M_\odot$

Radius: $13.7^{+2.6}_{-1.5}$ km (68%) (Miller et al. 2021) or $12.39^{+1.30}_{-0.98}$ km (Riley

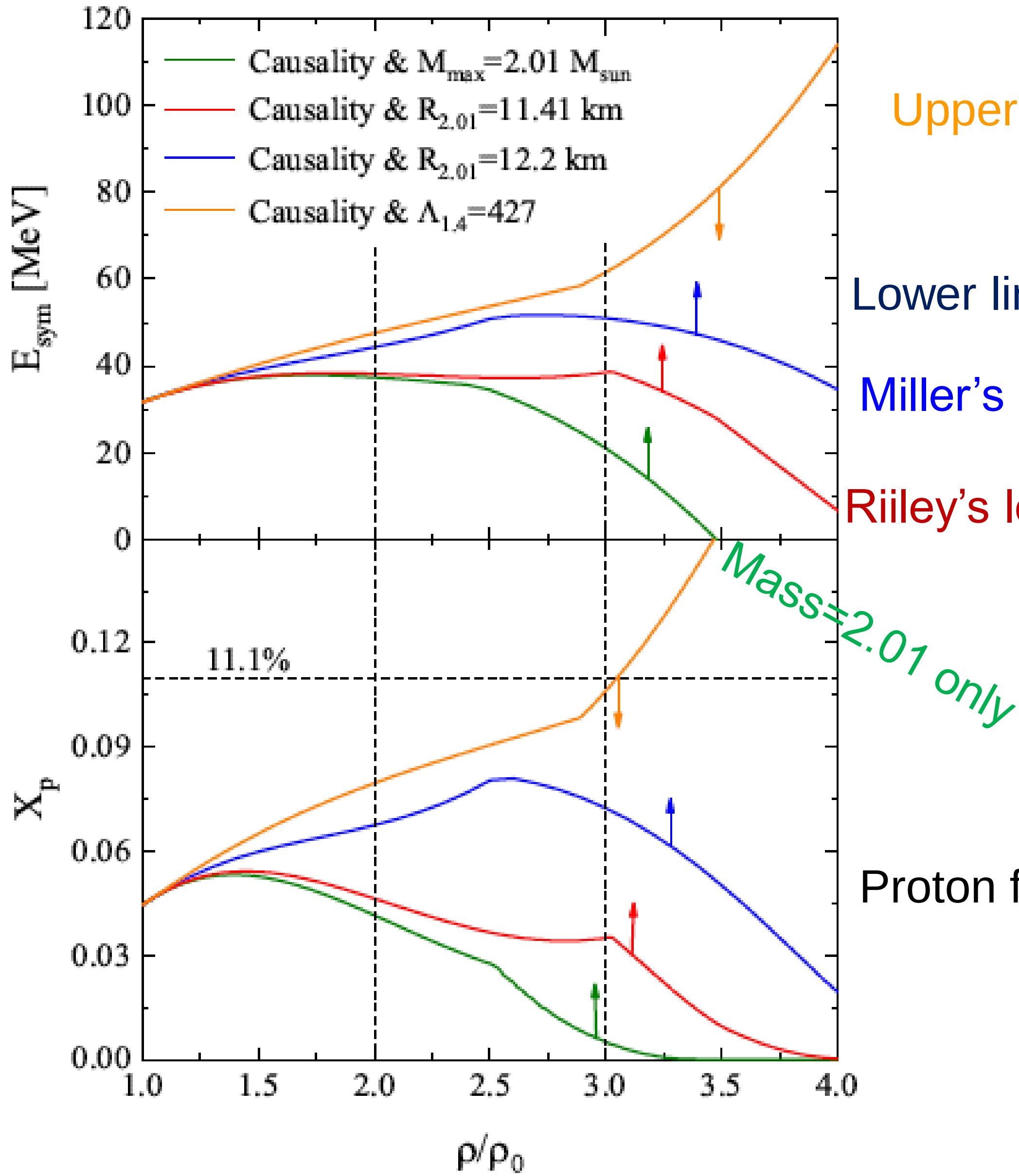

Upper limit on E_{sym} from GW170817

Lower limit on E_{sym} from PSR J0740+6620

Miller's lower radius

Riiley's lower radius

Proton fraction in PSR J0704+6620

N.B. Zhang and B.A Li
APJ 921, 111 (2021)

Effects of K_{sym} on isospin fractionation in heavy-ion collisions at intermediate energies

Bao-An Li, PRL 85, 4221 (2000)

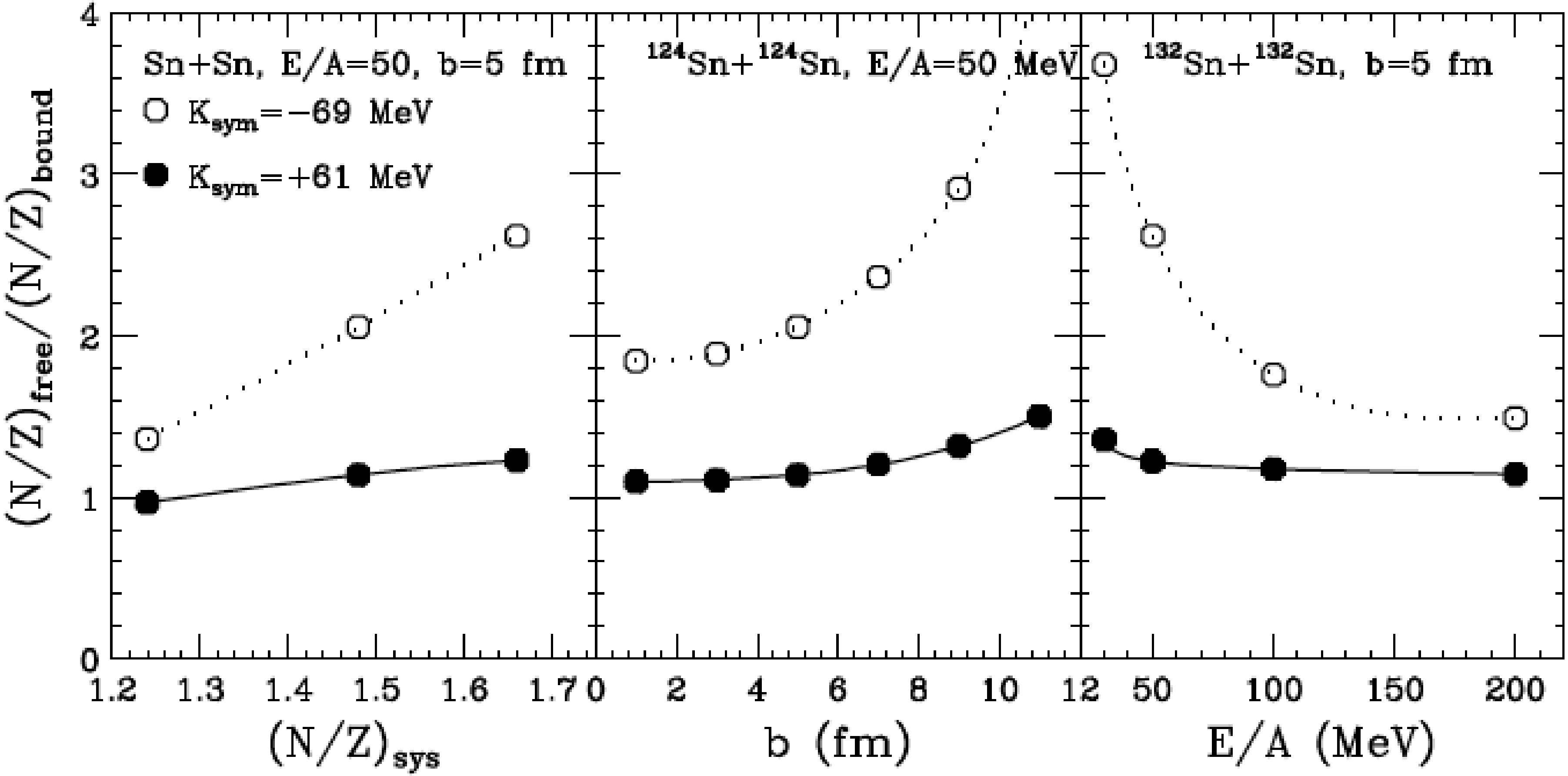

Neutron-proton differential flow

$$F_{n-p}(y) = \frac{1}{N(y)} \sum_{i=1}^{N(y)} p_{x_i} \tau_i,$$

τ_i=1 for neutrons and -1 for protons

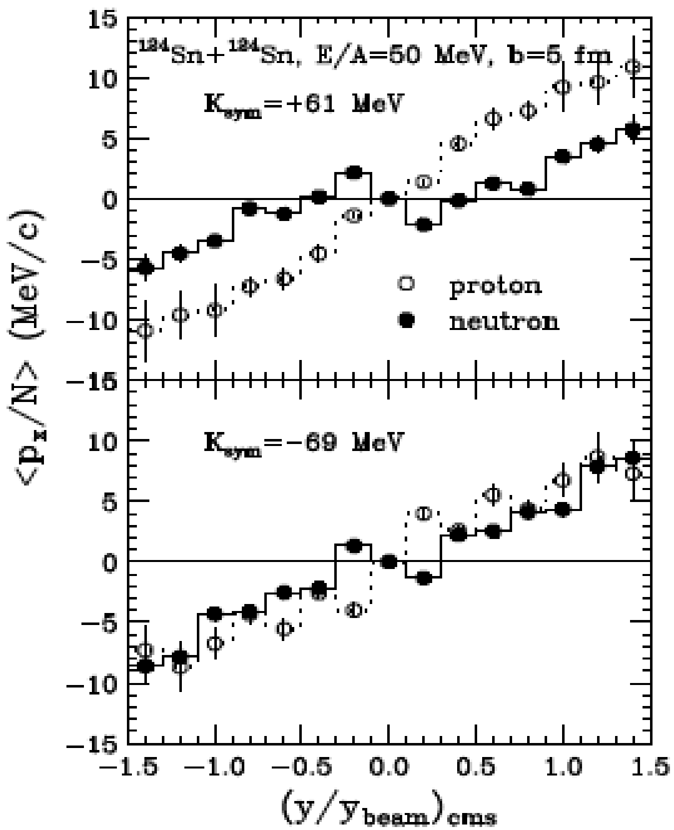

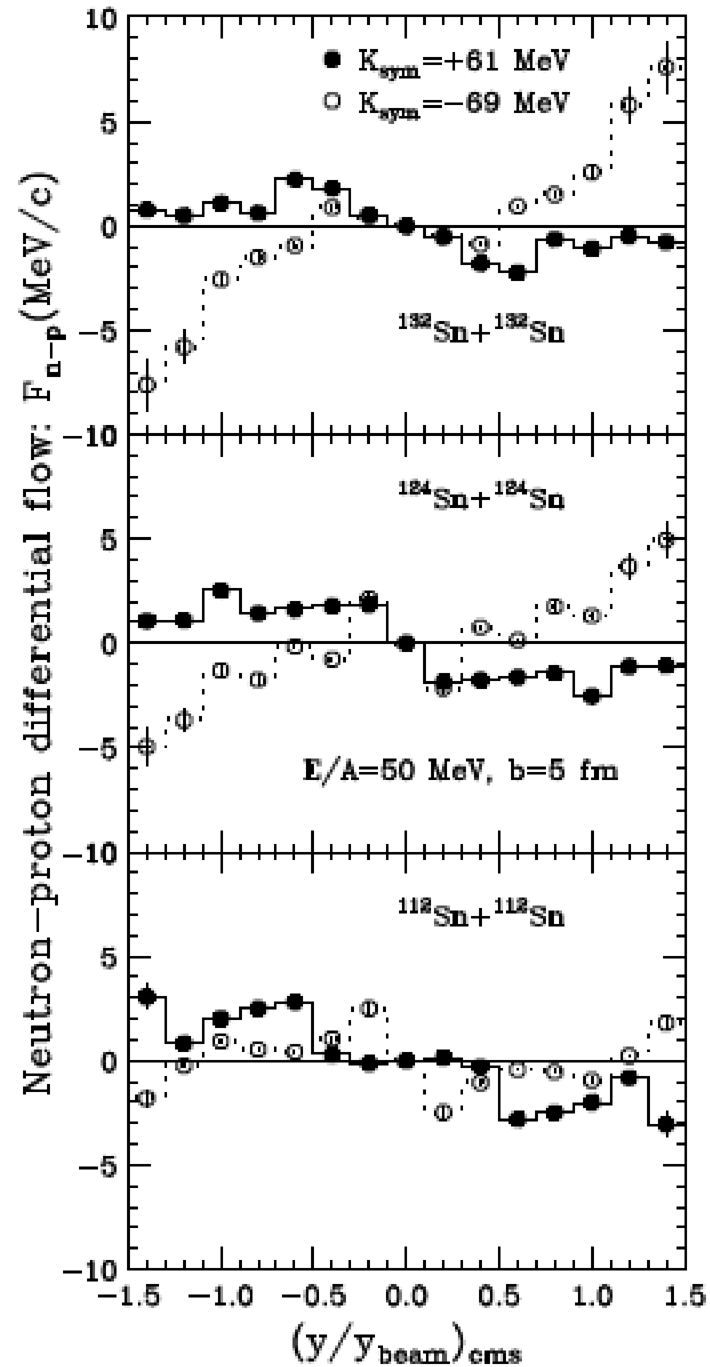

Bao-An Li, PRL 85, 4221 (2000)

Ratios of neutron to light charged particle ratios and elliptical flows from GSI
Dan Cozma, EPJA 54 (2018) 3

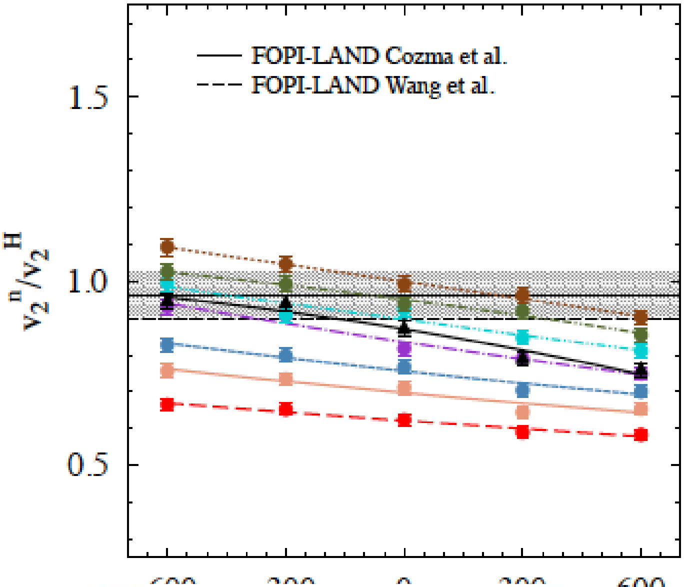

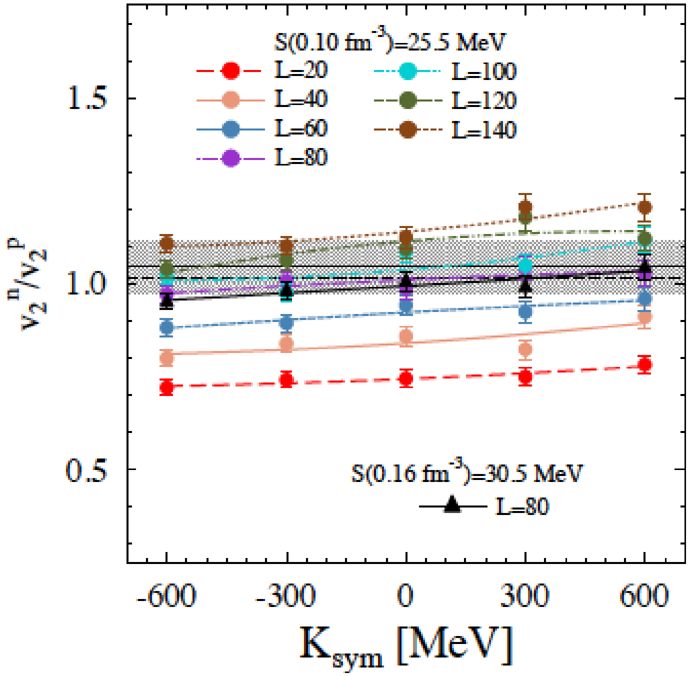

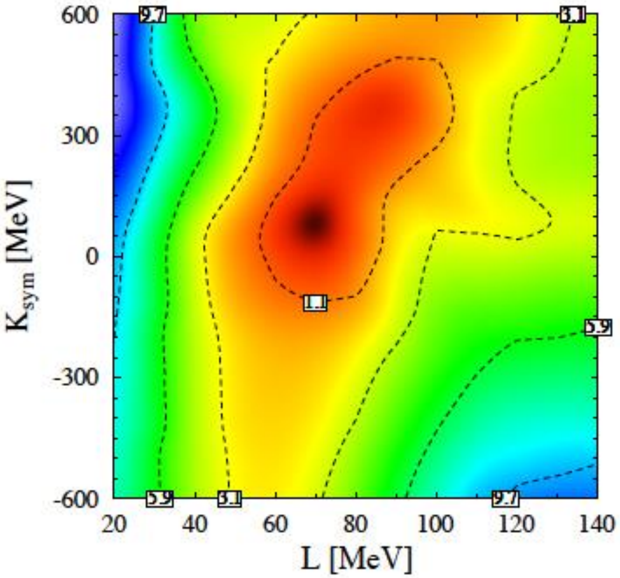

$$L = 85 \pm 22(\mathrm{exp}) \pm 20(\mathrm{th}) \pm 12(\mathrm{sys})\ \mathrm{MeV}$$
$$K_{sym} = 96 \pm 315(\mathrm{exp}) \pm 170(\mathrm{th}) \pm 166(\mathrm{sys})\ \mathrm{MeV}\,.$$

From Earth to Heaven: multi-messengers of nuclear EOS

(1) Significant progresses in understanding the role of isospin degree of freedom
(2) Many interesting issues to be resolved, correlations of SNM EOS and E_{sym}
(3) Truly multi-messenger approach to probe the EOS of dense neutron-rich matter
= astrophysical observations + terrestrial experiments + theories + your money and efforts +…..

INDRA--FAZIA

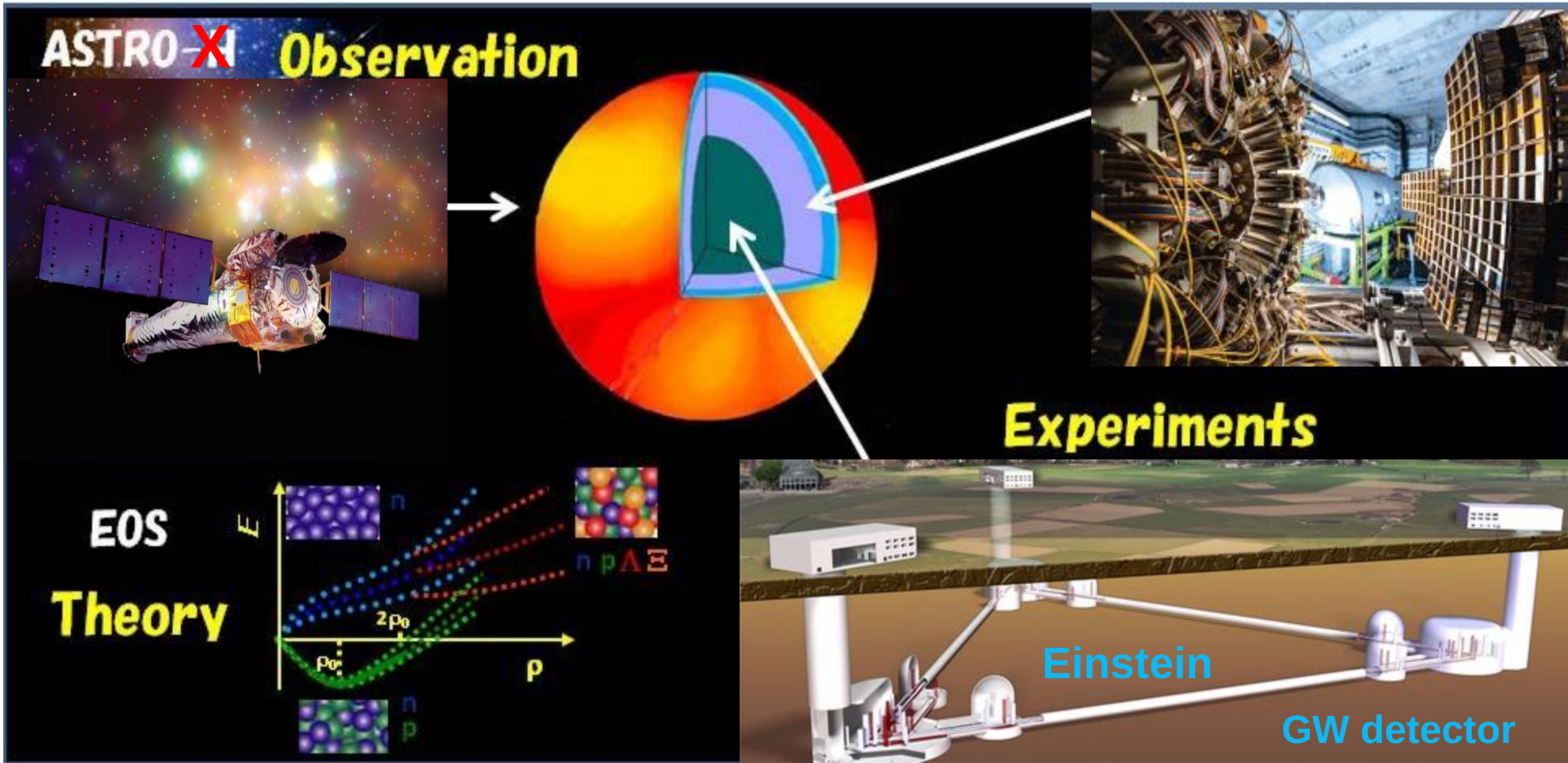


A road map towards determining the nature
and EOS of
tter
Collaboration is the key for success!
Gravity Theories
Reaction Theory
Shell Model
Continuum Shell Model
Neutron Stars
EOS
Collective Models
Algebraic Models
ab initio
GFMC, NCSM, CCM
NN and
many-nucleon
forces
EFT
MANY BODY
ASTRO
Under Construction
FAIR/Germany
RIKEN/Japan,
FRIB/USA
HIAF/China
ROAN/Korea
NICA/Russia
Transport
of neutrons,protons,pions
THEORY
EXPERIMENT
Heavy-ion Collisions
Ground-based
gravitational wave detectors